Coordination Chemistry Reviews, 60 (1984) 131–169
Elsevier Science Publishers B.V., Amsterdam – Printed in The Netherlands

THE ANGULAR OVERLAP MODEL FOR THE DESCRIPTION OF THE PARAMAGNETIC PROPERTIES OF TRANSITION METAL COMPLEXES

A. BENCINI
ISSECC, CNR, Florence (Italy)

C. BENELLI and D. GATTESCHI
Department of Chemistry, University of Florence, Florence (Italy)

(Received 6 January 1984)

CONTENTS

ABBREVIATIONS

acac	acetylacetone
acacen	*N*,*N*′-ethylenebis(acetylacetoneimine)
apy	1-phenyl-2,3-dimethyl-5-pyrazolone

bipy	2,2′-bipyridine
biquin	2,2′-biquinoline
5 Cl SALNdiethyl	5-chloro-*N*-β-diethylaminoethylsalicylideneimine
DAPSC	2,6-diacetylpyridine-bis(semicarbazone)
en	1,2-diaminoethane
iz	imidazole
L_N^+	*N*-ethyl-1,4-diazabicyclo[2.2.2]octonium
3 Me O SALen	*N*,*N*′-ethylenebis(3-methoxysalicylideneimine)
6-Me quin	6-methyl quinoline
mes	mesityl
MeTPMA	tris(3,5-dimethyl-1-pyrazolyl)methylamine
MeTPyEA	tris(3,5-dimethyl-1-pyrazolyl)ethylamine
Me$_6$tren	tris(2-dimethylaminoethyl)amine
N=C	*cis* endo *N*,*N*′-di(4-methylbenzilidene) meso 2,3-butane-diamine
NP$_3$	tris(2-diphenylphosphinoethyl)amine
NS$_3$	tris(2-tert-butylthioethyl)amine
p$_3$	1,1,1-tris(diphenylphosphinomethyl)ethane
pd	propane-1,3-diamine
PEt$_2$P	bis(diethylphenylphosphine)
phen	1,10-phenanthroline
picNO	4-methylpyridine-*N*-oxide
POOP	ethylene bis(oxyethylene)-bis(diphenylphosphine)
POP	oxy-diethylenebis(diphenylphosphine)
py	pyridine
PyNO	pyridine-*N*-oxide
pyr	pyrazine
pz	pyrazole
quin	quinoline
SALen	*N*,*N*′-ethylenebis(salicylaldimine)
SALNisopropyl	*N*-isopropylsalicylaldimine
SALNmethyl	*N*-methylsalicylaldimine
semicarb	semicarbazide
tdmmb	7,15-dihydro-7,9,13,15-tetramethylpyrido-2′,1′,6′ : 12,13,14 1,2,4,7,9,10,13 heptaazacyclo-pentadeca 3,4,5,6,7,8-*aklmn* 1,10 > phenanthroline
TMC	1,4,8,11-tetramethyl-1,4,8,11-tetraazacyclotetradecane
as-Et$_2$en	*N*,*N*-diethylethylenediamine
as-Me$_2$en	*N*,*N*-dimethylethylenediamine
s-Et$_2$en	*N*,*N*′-diethylethylenediamine
TMen	*N*,*N*,*N*′,*N*′-tetramethylethylenediamine
TCA	trichloroacetate

A. INTRODUCTION

The angular overlap model (AOM) [1] was originally developed as a simplification of the molecular orbital (MO) treatment of the electronic energies of transition metal complexes [2]. The model was developed, mainly through the work of Schäffer, as a different formalism for a ligand field model [3–13]. It has acquired increasing popularity [14–21] due to the chemical appeal of its parameters and the possibility of transferring them from one complex to another.

The AOM is well suited for calculating the energies of the *d–d* transitions without any restriction due to the symmetry of the complex. In fact, it can handle equally well the energies of either octahedral complexes or chromophores possessing no symmetry at all, the only limitations being in the number of parameters which are required. Although in principle the electronic spectra must reflect the actual symmetry of the complex, in practice, low-symmetry effects are hardly observed or recognized, due to the broadness and the overlap of the bands, and concepts such as "idealized" symmetry are widely used. For example, although the true symmetry of a complex may strictly speaking be only C_1, the spectra can reasonably be assigned using D_{4h} or perhaps O_h symmetry [22–24]. In this respect, there is not much hope of obtaining meaningful values for the AOM parameters.

On the other hand, paramagnetic properties, i.e. paramagnetic susceptibility and EPR spectra, are much more sensitive to low-symmetry effects and their calculation affords a meaningful testing ground for the AOM. A significant step in the calculation of the paramagnetic properties of low-symmetry transition metal complexes was made some years ago by Gerloch and McMeeking [25]. They suggested a procedure for the calculation of the paramagnetic susceptibility, and of the **g** tensor, in which no assumption need be made about the "effective" symmetry of the complex, or about the principal axes of the tensors. Everything can be calculated once the geometry and the relevant energy parameters are fixed. The values of the energy parameters are those which give the best fit to the experimental data. Owing to the large number of parameters which are required for a low-symmetry complex, it is always advisable to include in the fitting procedure as many experimental data as possible. In an ideal case, one should use single-crystal polarized electronic spectra and EPR spectra, as well as magnetic anisotropy data to fit the principal values and directions. Unfortunately, this procedure has rarely been followed and generally the calculated AOM parameters are the result of a fit only to a limited set of experimental results. Sometimes different sets of parameters may be calculated if different experimental properties are included in the analysis. When this occurs it is necessary to recalculate the AOM parameters taking into consideration all the available experimental data together.

Since many different applications of the AOM have been made, we felt it appropriate to collect in one place information about the techniques of calculation, not only of the paramagnetic susceptibilities, but also of the most important spin Hamiltonian parameters which are needed for the interpretation of the EPR spectra. Therefore in this article we propose briefly to review the foundation of the AOM; to show how calculations can be performed for different metal ions, including spin–orbit coupling effects; to consider the effect of an external magnetic field on the energy levels, and to calculate the **g**, **D**, **A** and $\boldsymbol{\chi}$ tensors. Finally, we will collect a set of experimental data, showing how it is possible to obtain consistent sets of AOM parameters from an analysis of the spectroscopic and magnetic properties. Although the analysis of one particular complex may be difficult, and may yield parameters which are not too significant, we are now in a position to have at least a rough idea of the range of values which can be expected, for example, for a chloride ion bound to a cobalt(II) ion. It is hoped therefore, that the values collected here will help people in assigning the spectral and magnetic properties of low-symmetry transition metal complexes. In particular, we hope that this review will be of use for the analysis of the spectra of metallo-enzymes and metallo-proteins. This is a field where, for some reason, the AOM has not yet been fully used, although potentially it could provide a very powerful investigative tool. In order to solicit activity in this area, we have added a section in which literature data on bio-inorganic systems are used and the analyses which have been performed with different approaches are translated into the AOM language.

B. THE ANGULAR OVERLAP MODEL

The angular overlap model is a ligand field model which gives parametrically the energies of the partially filled $d(f)$ shell of transition metal complexes through a first-order perturbation treatment using a basis of metal orbitals, without explicitly taking into account the ligand orbitals [4]. The central assumption of the method is that for a ligand on the Z axis the metal–ligand interaction is diagonal; therefore the matrix elements of the angular overlap operator, $\hat{\mathbf{A}}$, within a basis of $d(f)$ orbitals, can be expressed as

$$\langle \lambda i | \mathbf{A} | \lambda' j \rangle = \delta_{\lambda\lambda'} \delta_{ij} e_{\lambda i} \tag{1}$$

where $\lambda i = \sigma$, πs, πc, δs, δc, corresponds to the irreducible representations (and their components) of the $C_{\infty v}$ group. Usually, an explicit form is not given to the $\hat{\mathbf{A}}$ operator, although it can conveniently be expressed as

$$\hat{\mathbf{A}} = \sum_{e} \sum_{\lambda i} C_e^{\lambda i} | l^{\lambda} \rangle \langle l^{\lambda} | \tag{2}$$

where the sums are over ligand orbitals, l is the secondary quantum number, and $C_e^{\lambda_i}$ are appropriate coefficients.

Central to an appreciation of the value of the AOM is an understanding of the value of the e_{λ_i} parameters. The original derivation of the model [2] was from the Wolfsberg–Helmholz approximation [26] of the MO model, and within this scheme σ, πs, πc, etc. have their obvious chemical-sense meanings. So, for instance, $e_{\pi s}$ refers to the π interaction parallel to the y direction, and $e_{\pi c}$ refers to that parallel to x. This formal equivalence is widely used in order to reduce the number of parameters required to express the energies of the $d(f)$ orbitals. In general, both $e_{\delta s}$ and $e_{\delta c}$ are assumed to be zero, on the grounds that d ligand orbitals, which could interact with metal orbitals of these symmetries, should in any case give very little overlap. It is worth mentioning here that this assumption has recently been questioned on the basis of a comparison of AOM results with ab initio calculations [27]. Another commonly accepted assumption is that $e_\pi = 0$ for an sp^3 hybridized nitrogen atom, and experimental results seem to agree with this view [28,29].

Equation (1) does not imply that the symmetry of the ligand–metal interaction is cylindrical, as might occur with a halogen-like donor (Fig. 1a) since the sine, s, and cosine, c, components of π and δ can be different from each other. Equation (1) means that the symmetry of the M–L moiety is at least C_{2v}. In this group, z^2 and x^2-y^2 should be mixed, but since it is common practice, as mentioned above, to assume that $e_{\delta s} = e_{\delta c} = 0$, it may also be assumed that the off-diagonal element $e_{\sigma'\delta} = 0$.

A possible example of a metal–ligand interaction which does not have cylindrical symmetry is pyridine (Fig. 1b). The π interaction is expected to be significantly different only from the zero orthogonal to the aromatic plane, therefore $e_{\pi s} \neq 0$ and $e_{\pi c} = 0$, if the aromatic plane is parallel to the xz molecular plane. Ligands which behave like this are non-linearly ligating [29]. What happens for an interaction such as that depicted in Fig. 1c is less clear. In this case the maximum symmetry is C_s, but may be lower. Even in the upper limit, assuming that zx is the symmetry plane, the assumption of a

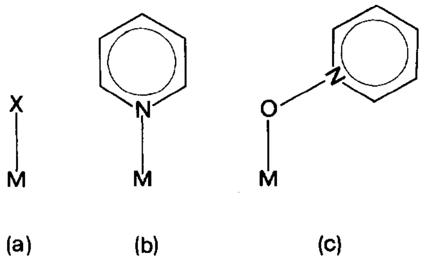

Fig. 1. Three different types of metal–ligand bonding interactions.

diagonal interaction seems to be questionable, since x^2-y^2, z^2, and xz span the same irreducible representation. In fact, in the σ and π labelling then loses significance. However, it is common practice to keep the validity of eqn. (1). This may not be too severe an assumption, as far as the energy differences among the metal orbitals are concerned. However, it may have relevant consequences in the evaluation of the tensor properties of the complexes **g**, $\boldsymbol{\chi}$, **D**, **A**, $\boldsymbol{\epsilon}$, etc. which are largely influenced by the admixture of orbitals possessing different spatial orientations. With the above assumptions, the maximum number of independent parameters for each ligand is three, namely e_σ, $e_{\pi s}$, $e_{\pi c}$.

The extension of eqn. (1) to the case of a ligand placed in a general direction in the metal-centred reference frame is made simply by considering how the overlap of the angular part of the $d(f)$ metal functions varies. This is the origin of the name of the model itself. Finally, it is assumed that the contributions from different ligands are additive. All these considerations are taken into account in the equation

$$\langle \mathrm{d}u|\mathbf{A}|\mathrm{d}v\rangle = \sum_N \sum_k \mathbf{F}_{uk}\mathbf{F}_{kv}e_k^N \tag{3}$$

where the N summation runs over all the ligands, the k summation over the five(seven) $d(f)$ orbitals and **F** is the angular overlap matrix, which is a function of the ligand coordinates. A suitable form of **F** for d orbitals is given in ref. 4, while for f orbitals it is given in refs. 30 and 31.

By using eqn. (3), it is possible to express the one-electron $d(f)$ energies for any cluster of ligands without making any assumption about the symmetry of the complex. It is possible, and often desirable, to use the ligand coordinates as found in the crystal structure determination. Therefore, "low-symmetry effects" are taken into account from the very beginning. Also, the choice of the molecular frame is absolutely arbitrary, although it is generally advisable to use a reference which corresponds to the symmetry of the complex, either true or idealized. The reason for this is obviously that of describing the computed states in the simplest possible way. The number of parameters required to describe the energies of the electronic transition depends on the number of independent ligands, i.e. ligands which are not related by symmetry operations of the molecule. Whether this number is larger than, equal to, or smaller than the number of independent experimental observables depends very much on the particular problem considered. For example, in an octahedral hexaquo-ion the highest possible symmetry is T_h, and the d orbitals split into two levels. Only one electronic transition is expected, but three AOM parameters are required for each water molecule, i.e. e_σ, $e_{\pi s}$ and $e_{\pi c}$.

In general, in order to have a meaningful set of values for the e_{λ_i}

parameters, one should obtain as much experimental information as possible. Therefore it is important not only to have available electronic spectra but also to use the several observables which can be obtained by employing external magnetic fields.

Recently, Woolley and Gerloch et al. suggested a parameterization scheme [18,32] according to which it is possible to decompose the environment of the metal ion into cells, which has some resemblance to the muffin-tin approximation of the $X\alpha$ potential [33]. In general each cell corresponds to a ligand, but this is not a necessary condition. In fact, if considering a square-planar complex it may be wise to include cells above and below the plane, not centred on any ligand, in order to have a more proper description of the electron density distribution of the complex. It is worth noting that this provides an alternative explanation to the well-known inadequacy of both ligand field and AOM methods to describe the electronic levels of square-planar complexes [34–36]. In fact, these models always result in too low an energy of the z^2 orbital; it is generally assumed that this behaviour is determined by the mixing of $4s$ orbitals into the d orbitals. Conversely, in the approach suggested by Gerloch et al. [32] this behaviour is determined by the residual electron density on the z axis and can be accounted for by using e_λ parameters for the "empty" cells located there.

C. ANGULAR OVERLAP/SPIN–ORBIT COUPLING CALCULATIONS

The energy levels for a many-electron system must be calculated by diagonalizing the Hamiltonian

$$\hat{\mathbf{H}} = \hat{\mathbf{A}} + \sum_{i<j} \frac{e^2}{r_{ij}} + \sum_{i} \xi_i k \hat{\mathbf{l}}_i \cdot \hat{\mathbf{s}}_i \tag{4}$$

on a suitable chosen basis. $\hat{\mathbf{A}}$ is the angular overlap operator, the second term is the electron repulsion operator, and the third term is the spin–orbit coupling operator. ξ_i is the one-electron spin–orbit coupling constant and the sums are over all the electrons of the configuration. A convenient basis set, for a given $d^n(f)$ congifuration, is described by functions of the type

$$| \alpha l L S J M_j \rangle \tag{5}$$

where $l = d, f$; L, S, J and M are the usual angular momentum quantum numbers and α represents all the additional quantum numbers required to identify a given function.

In general, for d metal ions, it is not advisable to split eqn. (4) into components and find the eigenvalues and eigenvectors of successive perturbations, as was the case in the weak-field, strong-field and rare-earth schemes [37]; rather, it is better to diagonalize the full matrix of eqn. (4). Of course, the ease with which this can be accomplished depends on the dimension of the basis, which in turn depends on the number of $d(f)$ electrons.

While relatively speaking it is not time consuming to calculate the ligand field/electron repulsion/spin–orbit coupling energy levels of d^1 or d^2 systems, for the d^3 configuration a 120×120 matrix should be diagonalized and for d^5 the order of the matrix increases to 252. For systems above d^3 it is therefore preferable to use smaller bases, if the physical problem allows one to eliminate from the calculation some set of basis functions.

If one is interested in the properties of, for example, high-spin cobalt(II) complexes, then it is usually a fair approximation to include only quartet states in the calculation, thus reducing the order of the basis from 120 to 40. Conversely, in the calculation of the molecular properties of low-spin cobalt(II) states, one might use the remaining 80 doublet states. However, this would not in general be a good approximation. Very high energy states should be included, which presumably are of little importance in determining the ground-state properties, yet some of the quartet states are quite close to the ground state. It is necessary to include these as well, in order to calculate molecular properties [38]. Therefore it seems advisable in this case to start from a strong field approach and select the lowest-energy states in this basis.

When considering many-electron configurations it is necessary to introduce an additional number of parameters, compared to the one-electron case, in order to take into account covalency effects which are included only implicitly in the AOM. If we regard the AOM as a parameterized MO treatment, then we must expect different β values of the nephelauxetic parameter when considering different orbitals. Jørgensen showed that for octahedral symmetry three different β values are needed, which he called β_{33}, β_{35}, and β_{55} [39], while in an MO description of a complex lacking any symmetry there are ten different βs [40]. It is apparent that this makes the task of obtaining meaningful values of the parameters from the experiment an impossible one. Therefore it is common practice to use one β value, i.e. assuming spherical symmetry as far as the electron repulsion is concerned.

When spin–orbit coupling and electronic Zeeman effects are taken into account, another parameter must be included, the Stevens' orbital reduction factor, k [41], which is intended to reduce the expectation value of the orbital momentum operator according to $k\mathbf{L}$, where $0 < k < 1$. Here, the problem is whether k should be isotropic, or vary according to the component of $\mathbf{L}$ under consideration [42], giving three different values, k_x, k_y, and k_z. EPR spectroscopists have often been obliged to use anisotropic k values, although it seems desirable to use an isotropic value of k as far as possible to reduce the number of parameters to a minimum.

Finally, another quantity, the spin–orbit coupling constant, $\zeta = \langle d \,|\, \xi(r) \,|\, d \rangle$, is expected to be reduced in such a way as to be no longer spherical, although it seems desirable to use a spherical ζ for the sake of simplicity.

D. ELECTRONIC SYSTEMS IN MAGNETIC FIELDS

When a transition metal complex containing unpaired electrons is introduced into a magnetic field, other terms must be added to the Hamiltonian in eqn. (4). Thus

$$\hat{\mathbf{H}}_{\mathrm{M}} = \mu_{\mathrm{B}}\mathbf{B}\cdot(g_e\hat{\mathbf{S}} + \hat{\mathbf{L}}) - \mu_N g_N \mathbf{B}\cdot\hat{\mathbf{I}}_N + \ldots \tag{6}$$

where $\mathbf{B}$ is the external magnetic field vector; μ_{B} is the Bohr magneton and μ_N is the nuclear magneton; g_e and g_N are the electron and nuclear g factors, respectively. Other terms must be added to the Zeeman electronic and nuclear Hamiltonians, such as those relative to fine and hyperfine magnetic interactions, which are not field dependent but are of the same order of magnitude as $\mathbf{H}_{\mathrm{M}}$.

Taking into account all these interactions gives rise to a series of observables obtainable with different techniques, e.g., magnetic susceptibility, EPR and ENDOR spectroscopy, MCD spectroscopy, NMR spectroscopy and magnetically perturbed Mössbauer spectroscopy.

The main observables are: the magnetic susceptibility, χ, which relates the external applied magnetic field $\mathbf{B}$ to the resulting magnetization; the electronic $\mathbf{g}$ tensor, which measures the field-dependent splitting of the electronic levels; the zero-field splitting tensor, $\mathbf{D}$, which depends on the splitting of the S levels in the absence of an external magnetic field; and the magnetic hyperfine tensor, $\mathbf{A}$, which is related to the interaction between the electron spin and the nuclear spin, etc. In the following sections we will illustrate these quantities and show how they can be calculated using the AOM formalism.

In order to refer to all these quantities in a unitary way it is useful to define a spin Hamiltonian, which only operates on spin coordinates, and which gives the same results as the true Hamiltonian in eqn. (6) when a suitable basis of spin functions is chosen [44,45]

$$\mathbf{H} = \mathbf{B}\cdot\mathbf{g}\cdot\hat{\mathbf{S}} + \hat{\mathbf{S}}\cdot\mathbf{D}\cdot\hat{\mathbf{S}} - \sum_N \hat{\mathbf{I}}_N\cdot\mathbf{g}_N\cdot\mathbf{B} + \sum_N \hat{\mathbf{I}}_N\cdot\mathbf{A}_N\cdot\hat{\mathbf{S}} + \ldots \tag{7}$$

The basis of the $2S+1$ spin functions on which the Hamiltonian (7) operates may or may not coincide with the true spin S of the system. Essentially the number of functions which must be included in the calculation depends on the number of states which are populated at the temperature at which the experiment is performed. In order to make this statement clear it is useful to give an example.

Octahedral high-spin cobalt(II) complexes have a $^4T_{1g}$ ground state: therefore the "true" spin for these systems is 3/2. Spin–orbit coupling introduces some $S = 1/2$ character into these functions, but loosely speaking we can still consider a spin quartet ground state. Now, due to fast relaxation [46], the EPR spectra can be measured only at very low temperatures, < 20 K. At these temperatures only the lowest Kramers' doublet is populated, so that the simplest way of interpreting the experimental data is by using an effective spin Hamiltonian, operating on a spin basis of $S = 1/2$, corresponding to the fictitious degeneracy of the ground level.

E. THE **g** TENSOR

The **g** tensor is experimentally best obtained from analysis of the EPR spectra of the complexes, although indirect information can also be obtained through magnetic susceptibility measurements.

Actually, **g** is not a tensor, although it is often referred to as such, but $\mathbf{g}^2 = \tilde{\mathbf{g}} \cdot \mathbf{g}$ is. One has to specify six components, g^2_{xx}, g^2_{xy}, g^2_{xz}, g^2_{yy}, g^2_{yz}, g^2_{zz} in order to define the tensor itself. It is always possible, by properly choosing the reference frame for the tensor, to make it diagonal, i.e. by setting all the ij components, $i \neq j$, equal to zero. The diagonal values are called principal values and the corresponding directions are thus the principal directions of the tensor. Both principal values and principal directions of $\mathbf{g}^2$ may be obtained through the analysis of single-crystal EPR spectra. They represent a good testing ground for the AOM calculations, in the sense that these can be considered to be satisfactory only if they are able to reproduce both sets of data. Following our previous discussion on the number of parameters and experimental data, it is worth noting that the $\mathbf{g}^2$ tensor yields six data points.

In order to calculate $\mathbf{g}^2$, within the AOM scheme, it is necessary to diagonalize within a suitable basis the Hamiltonian matrix of eqn. (4), which does not include field-dependent terms. Then one has to focus on the lowest states and to apply the (electronic) Zeeman Hamiltonian (6). In the case of a ground multiplet, well separated in energy from all the others, i.e. with excited levels at energies much larger than kT, $\mathbf{g}^2$ can be computed according to the relation [25,38]

$$g^2_{\alpha\beta} = \frac{\sum\limits_{i}\sum\limits_{k} \langle i | \hat{\mu}_\alpha | k \rangle \langle k | \hat{\mu}_\beta | i \rangle}{\sum\limits_{M_S = +S}^{-S} M_S^2} \tag{8}$$

where $| i \rangle$ and $| k \rangle$ are the spin–orbit functions belonging to the ground multiplet, the sums are over all the functions of the multiplet,

$$\hat{\mu}_\alpha = \mu_B \mathbf{B} \cdot \sum_i (\hat{\mathrm{l}}_{i\alpha} + g_e \hat{\mathrm{s}}_{i\alpha}),$$

and α and β are Cartesian components. The S value in the denominator in eqn. (8) is chosen in such a way that $2S+1$ equals the total multiplicity of the ground multiplet. The generally non-diagonal $\mathbf{g}^2$ tensor calculated through eqn. (8) can be made diagonal using standard techniques yielding the principal values and directions. In general, the diagonal reference frame does not correspond to the molecular reference frame within which the AOM matrix is computed unless symmetry requires it.

The computed $\mathbf{g}^2$ tensor is the true $\mathbf{g}^2$ tensor if the degeneracy of the lowest multiplet is true spin degeneracy, otherwise it is the effective $\mathbf{g}^2$ tensor defined within the effective spin basis S, as discussed in the previous section. A useful example to make this point clear comes from the EPR spectra of high-spin cobalt(II) complexes. Tetrahedral complexes have a $^4A_2$ ground state with excited states at energies larger than 10^3 cm^{-1} [22,46]. In rigorous tetrahedral symmetry the quartet is not split by spin–orbit coupling, so that the multiplicity of the ground manifold is identical to the spin multiplicity. The quartet, however, is split by interaction with the magnetic field, and the experimental g values and those computed using eqn. (8) are true g values. If the symmetry is lower than tetrahedral then the ground quartet is split into two Kramers' doublets, whose separation is typically of the order of 10^2–10^1 cm^{-1} [38,46]. If only the lowest doublet is populated the EPR spectra will be those of a spin doublet. Both the experimental g values and those calculated using eqn. (8) with the sum extended only to the two lowest-energy functions will be effective g values and not true g values, therefore allowing a direct comparison between calculated and observed values. Sometimes it may also be useful to have available the true g values. These can easily be computed using eqn. (8), provided that the sum is extended to the first excited doublet.

An alternative approach to calculating the "true" g tensor is perturbative. In this case, $\mathbf{g}$ is computed using the relations [47]

$$g_{\alpha\beta} = g_e \delta_{\alpha\beta} + 2\lambda\, \Lambda_{\alpha\beta} \tag{9}$$

where λ is the spin–orbit coupling constant within the ground term and

$$\Lambda_{\alpha\beta} = \sum_n{}' \frac{\langle G | L_\alpha | n \rangle \langle n | L_\beta | G \rangle}{E_n - E_G} \tag{10}$$

where $|G\rangle$ is the ground state, $|n\rangle$ is an excited state, and the sum is extended over all the excited states. The functions in this case are the ligand field functions, before the spin–orbit calculation, since spin–orbit coupling is introduced as a perturbation.

There will be correspondence between the computed g values and those obtained experimentally from analysis of the EPR spectra if the multiplet, which is degenerate in the absence of the field, is separated from the excited levels by an energy which is large compared to kT. In general, this will apply to all systems with one unpaired electron, which have an orbitally non-degenerate ground state, to complexes with an odd number of electrons experiencing large zero-field splittings, and also to systems with an odd number of electrons and orbitally degenerate ground states.

For systems in which more than one multiplet belonging to the same spin S is thermally populated, the g values must be computed by extending the summation in eqn. (8) to all the states which are populated.

A comparison with experiment also demands the calculation of the zero-field splitting tensor, **D**, which will be outlined in the next section.

A complication which may arise in the interpretation of the EPR spectra of magnetically non-dilute systems is that intermolecular exchange interactions may wipe out the inequivalence of different magnetic sites in the unit cell, yielding an average **g** tensor [48]. In a monoclinic cell, for instance, the two molecules related by the C_2 axis will, in general, have different orientations in a given crystal setting. If no intermolecular exchange interaction is operative, two signals will be obtained in a general single-crystal experiment, but if the exchange interaction is larger than the frequency difference of the two signals, then only one signal will be obtained, in the average position. The present model can also be used to treat this case. It suffices to calculate the **g** tensors of the various symmetry-related sites and to calculate the crystal-averaged **g** tensor, which will then be compared with experiment.

In order to calculate the $\mathbf{g}^2$ tensor of a complex, no other adjustable parameter is added to those required for a complete AOM/spin–orbit coupling calculation.

F. THE D TENSOR

The zero-field splitting tensor, **D**, is a true tensor, which is usually taken as traceless. In the spin Hamiltonian formalism, it is an electron spin–electron spin interaction, $\mathbf{H} = \hat{\mathbf{S}} \cdot \mathbf{D} \cdot \hat{\mathbf{S}}$, but for transition metal complexes, it is essentially determined by spin–orbit coupling effects [49]. As such, the splitting of the levels which formally originate from the same spin multiplet in the absence of the magnetic field is easily obtained from the energies of the levels known through AOM/spin–orbit coupling calculations. However, owing to its definitions through the spin Hamiltonian (7), which is intrinsically a perturbation Hamiltonian, the best way to calculate **D** is to use perturbative formulae. In this scheme a ligand field calculation is performed and the tensor is obtained from the relation

$$\mathbf{D}_{\alpha\beta} = \lambda^2 \Lambda_{\alpha\beta} \tag{11}$$

where λ and $\Lambda_{\alpha\beta}$ were defined in eqn. (10). It is apparent that, at this level of approximation, both $\mathbf{g}^2$ and $\mathbf{D}$ are diagonal in the same reference frame.

When studying systems with $S > 3/2$, the zero-field splitting is not described just by the $\hat{\mathbf{S}} \cdot \mathbf{D} \cdot \hat{\mathbf{S}}$ term of the spin Hamiltonian; biquadratic spin terms of the type shown below must also be included [49]

$$\frac{a}{6}\hat{\mathbf{S}}_x^4 + \hat{\mathbf{S}}_y^4 + \hat{\mathbf{S}}_z^4 - \frac{J(S+1)(3S^2+3S-1)}{5} + \frac{F}{180} 35\,\hat{\mathbf{S}}_z^4 - 30S(S+1)\hat{\mathbf{S}}_z^2$$
$$+25\,\hat{\mathbf{S}}_z^2 + 6S(S+1) \tag{12}$$

Although spin–orbit coupling presumably is involved in the origin of these terms, they are generally fairly small, and to our knowledge no serious attempt has been made to calculate the parameters a and F within a ligand field framework.

G. THE A TENSOR

The metal hyperfine tensor can easily be calculated within a ligand field formalism. However, ligand hyperfine tensors cannot be calculated, owing to the neglect of ligand functions inherent to the model.

The metal hyperfine tensor components, A_{ij}, are given by the sum of three terms: the contact, the spin dipolar, and the orbit dipolar [50]. The contact term depends on the unpaired spin densities on the nucleus. As such it is determined by the fraction of unpaired spins present in the s metal orbitals. It is not calculated in the ligand field scheme but is used as a parameter. In general its value is assumed, without much foundation [51], to differ little from the value observed in the corresponding free ion, possibly reducing it to a factor similar to that used for other covalency effects. This term is isotropic, and is often expressed as

$$A_{xx}^{\text{con}} = A_{yy}^{\text{con}} = A_{zz}^{\text{con}} = -P\kappa \tag{13}$$

where $P = g_e g_N \mu_B \mu_N \langle r^{-3} \rangle_{\text{av}}$ and κ is the Fermi contact constant; r is the electron–nucleus distance. $X\alpha$ calculations on tetrahedral $CuCl_4^{2-}$ ions showed that P for ^{63}Cu, which is usually assumed to be 360×10^{-4} cm^{-1}, or slightly smaller, can be as high as 440×10^{-4} cm^{-1}, thus explaining the unusually low $A_{\parallel}$ values seen in the EPR spectra of tetrahedral copper(II) complexes [38]. Useful reference values for P and κ in first-row transition metal ions are available [52].

The spin dipolar and orbit dipolar terms originate from the through-space magnetic interaction between the electron spin and orbit, respectively, and the nuclear spin. Convenient forms for these interactions are provided by the Hamiltonian [53]

$$\hat{\mathbf{H}} = P'\hat{\mathbf{S}}^* \cdot \mathbf{I} \tag{14}$$

where $P' = g_e g_N \mu_B \mu_N$; $\hat{\mathbf{I}}$ is the nuclear spin operator, and $\hat{\mathbf{S}}^*$ is given by

$$\begin{aligned}
\hat{\mathbf{S}}_x^* = \Big\{ & -(2\pi^{1/2}/5^{1/2}r^3)Y_2^0\hat{\mathbf{S}}_x + \left[3(2\pi)^{1/2}/(15)^{1/2}r^3\right](Y_2^2 + Y_2^{-2})\hat{\mathbf{S}}_x \\
& + \left[3(2\pi)^{1/2}/(15)^{1/2}r^3\right] i(Y_2^{-2} - Y_2^2)\hat{\mathbf{S}}_y \\
& + \left[3(2\pi)^{1/2}/(15)^{1/2}r^3\right](Y_2^{-1} - Y_2^1)\hat{\mathbf{S}}_z + \hat{\mathbf{I}}_x r^{-3}\Big\} \\
\hat{\mathbf{S}}_y^* = \Big\{ & -(2\pi^{1/2}/5^{1/2}r^3)Y_2^0\hat{\mathbf{S}}_y - \left[3(2\pi)^{1/2}/(15)^{1/2}r^3\right](Y_2^2 + Y_2^{-2})\hat{\mathbf{S}}_y \\
& + \left[3(2\pi)^{1/2}/(15)^{1/2}r^3\right] i(Y_2^{-2} - Y_2^2)\hat{\mathbf{S}}_x \\
& + \left[3(2\pi)^{1/2}/(15)^{1/2}r^3\right] i(Y_2^{-1} + Y_2^1)\hat{\mathbf{S}}_z + \hat{\mathbf{I}}_y r^{-3}\Big\} \\
\hat{\mathbf{S}}_z^* = \Big\{ & (4\pi^{1/2}/5r^3)Y_2\hat{\mathbf{S}}_z + \left[3(2\pi)^{1/2}/(15)^{1/2}r^3\right](Y_2^{-1} - Y_2^1)\hat{\mathbf{S}}_x \\
& + \left[3(2\pi)^{1/2}/(15)^{1/2}r^3\right] i(Y_2^1 + Y_2^{-1})\hat{\mathbf{S}}_y + \hat{\mathbf{I}}_z r^{-3}\Big\}
\end{aligned} \tag{15}$$

where y_e^m are spherical harmonics.

A, like **g**, is not a true tensor, while $\mathbf{A}^2$ is. The latter can be calculated [53] according to

$$\mathbf{A}^2 = \frac{\sum\limits_i \sum\limits_k \langle i | \mathbf{S}_\alpha^* | k \rangle \langle k | \hat{\mathbf{S}}_\beta^x | i \rangle}{\sum\limits_{m=1}^{2S+1} m^2} \tag{16}$$

where the symbols have the same meaning as in eqn. (8). The same considerations apply to $\mathbf{A}^2$ as to $\mathbf{g}^2$: the calculated $\mathbf{A}^2$ will be "true" or "effective" whether or not the multiplicity of the ground state corresponds to the spin multiplicity. In order to compare with experiment, the contact term, defined in eqn. (13), must be added to the $\mathbf{A}^2$ tensor calculated using eqn. (16). From the point of view of the number of parameters, the calculation of $\mathbf{A}^2$ requires the introduction of two additional ones, namely P and κ.

H. THE χ TENSOR

The paramagnetic susceptibility χ is a tensor defined through the relation

$$\mathbf{M} = \chi\mathbf{B} \tag{17}$$

where **B** is the external magnetic field and **M** is the resulting magnetization. In molecular terms the susceptibility can be defined as

$$\chi_{\alpha\beta} = -\frac{N}{\mathbf{B}_\beta}\,\frac{\sum\limits_i \frac{E_i}{\mathbf{B}_\alpha}\exp(-E_i/kT)}{\sum\limits_i \exp(-E_i/kT)} \tag{18}$$

where E_i is the energy of the ith thermally populated level and N is Avogadro's number. Equation (18) shows the temperature dependence of the paramagnetic susceptibility.

The most correct approach for obtaining χ would be to calculate the matrix of the Hamiltonian including the Zeeman interaction, then to evaluate the first derivatives and consequently χ. Although conceptually simple, this approach is computationally rather difficult, and only recently have serious attempts been made to exploit it fully [54]. In particular, a procedure has been described which employs a least-squares analysis to obtain the best-fit values of the ligand-field parameters [54].

In practice, it has been customary to use an approximate expression called the van Vleck approximation [55]. Central to this scheme is the assumption that the energy levels E_i can be expanded in a series

$$E_i = E_i^0 + E_i^{(1)}B + E_i^{(2)}B^2 + \ldots \tag{19}$$

which is converging sufficiently fast that the perturbation expansion can be terminated at second order and finally, that all energy changes due to the field are small compared with kT. Therefore eqn. (19) will be a reasonable approximation of E_i at high temperatures provided the field at which the measurement is made is small enough .to avoid paramagnetic saturation effects.

Using the van Vleck approximation, the magnetic susceptibility tensor can be written [25] as

$$\chi_{\alpha\beta} = \frac{\mathcal{N}}{Z}\sum_i\sum_k \langle i|\mu_\alpha|k\rangle\langle k|\mu_\beta|i\rangle/kT \\ - \sum_j \frac{(\langle i|\mu_\alpha|j\rangle\langle j|\mu_\beta|i\rangle + \langle i|\mu_\beta|j\rangle\langle j|\mu_\alpha|i\rangle)}{E_i^0 - E_j^0} \tag{20}$$

where $Z = \Sigma \exp(-E_i^0/kT)$; the i and k summations have exactly the same meaning as in eqn. (8); the j summation is extended to all states which are not thermally populated. Gerloch has sugggested methods of calculating χ on a computer in a fast and efficient way [25]. Single-crystal measurements are really needed for magnetic susceptibility. The reader interested in magnetic anisotropy measurements is referred to some excellent articles [56–58].

From experiment, one obtains the crystal magnetic susceptibility, which corresponds to the molecular magnetic susceptibility only when there is one magnetic site in the unit cell. This occurs in triclinic crystals, and, for higher-symmetry cells, only in the case when the site symmetry of the molecular site corresponds to the symmetry of the cell. Since eqn. (20) is a molecular property, it is necessary to apply to χ the symmetry operations of the cell in order to calculate χ for all the independent sites, and then to evaluate the crystal average. This procedure is identical to that outlined for the $\mathbf{g}^2$ tensor in the case of exchange-narrowing of the signals.

From the above discussion, it is apparent that there is a limitation in the procedure for obtaining meaningful AOM parameters from the magnetic susceptibility data alone: since one has a crystal average of molecular properties, in principle infinite combinations of molecular χ can give the same average. It usually is possible to restrict the choice to very few cases, or to one, owing to the requirement of physical significance of the solution; nevertheless, some ambiguity may be present. One example is that of $[Co(MePh_4A_sO)_4NO_3](NO_3)$. This complex was reported to be tetragonal [59], with the cobalt ion lying on a C_4 axis. The temperature dependence of the magnetic susceptibility was analysed on this assumption, and the relevant ligand-field parameters calculated [60]. However, single-crystal EPR spectra recorded at 4.2 showed that the symmetry of the cobalt(II) complex is definitely lower than axial, and only the crystal average is indeed tetragonal [61]. Since the effects of static or dynamic disorder in crystals, which make the symmetry of the complex different from that apparent from X-ray crystal-structure determination, are relatively common [62–68], extreme caution should always be exercised whenever the experimental technique used is sensitive only to crystal averages of molecular properties.

Indeed, EPR spectroscopy and magnetic susceptibility measurements are very complementary techniques, and both should be used in order to obtain meaningful images of the nature and the order of the lowest-lying energy levels of transition metal complexes. Unfortunately, the two techniques have been used together only rarely, and some additional effort in this field is extremely desirable.

I. SURVEY OF EXPERIMENTAL RESULTS

In the following sections are collected the values of the AOM parameters for selected classes of ligands. In general, we have used the data which were obtained from the analysis of either electronic spectra or magnetic susceptibility measurements, and EPR spectra, although in a few cases, where the reported values appeared to be significant, we show parameters obtained through only one set of data.

In Tables 2–9 are collected the AOM values and also the metal–ligand distance, since this is an important variable which determines the value of e_{λ_i}. It is worth mentioning here that in the early stage of development of the AOM several attempts were made to reduce the number of independent parameters using relations of the type [14,16,69,70]

$$e_{\lambda_i} = kS_\lambda^2 \tag{21}$$

where S_λ is the diatomic metal–ligand orbital, and k is a proportionality constant. Equation (21) has been used either for expressing e_π as a function of e_σ and of the ratio S_π^2/S_σ^2, or to correct for the distance. Owing to the large uncertainties associated with the functions used for metal and ligand orbitals, their dependence on the effective charge, and the rather little significance of using functions which are useful in an MO treatment for a ligand field model, this procedure is now rarely used. The problem now is mainly one of obtaining more experimental data, rather than that of reducing the number of parameters.

Since the classic ligand field parameters are often reported in the literature, it is useful to give the equivalence between these and the AOM parameters for linearly ligating ligands. Some useful relations are given in Table 1.

(i) Halogens

The halogen ligands require only two parameters, e_σ and e_π, and, owing to the large number of complexes in which they are present, afford a large number of examples. In Table 2 are given e_σ, e_π, e_π/e_σ and metal–ligand distances for several complexes, with different metal ions, and different stereochemistries.

TABLE 1

Relations among common ligand field and angular overlap parameters [a]

$$I_2 = (7/2)Cp = e_\sigma + e_\pi$$

$$I_4 = 6Dq = (9/5)e_\sigma - (12/5)e_\pi$$

$$Cp = (2/7)I_2 = (2.7)e_\sigma + (2.7)e_\pi$$

$$Dq = (1/6)I_4 = (3/10)e_\sigma - (4/10)e_\pi$$

$$e_\sigma = (4/7)I_2 + (5/21)I_4 = 2Cp + (10/7)Dq$$

$$e_\pi = (3/7)I_2 - (5/21)I_4 = (3/2)Cp - (10/7)Dq$$

[a] The symbols are defined in refs. 16, 60 and 71.

TABLE 2

Angular overlap and structural parameters for halogen complexes

Compound	e_σ^{X} [a]	e_π^{X} [a]	e_π^X/e_σ^X	Ref.	Metal–ligand distance [b]	Ref.
Pr^{3+} in $LaCl_3$	235	58	0.25	30		
Nd^{3+} in $LaCl_3$	257	71	0.28	30		
Pm^{3+} in $LaCl_3$	271	85	0.31	30		
Sm^{3+} in $LaCl_3$	236	63	0.27	30		
Eu^{3+} in $LaCl_3$	254	56	0.22	30		
Gd^{3+} in $LaCl_3$	253	69	0.27	30		
Tb^{3+} in $LaCl_3$	232	90	0.39	30		
Dy^{3+} in $LaCl_3$	252	104	0.41	30		
Ho^{3+} in $LaCl_3$	243	99	0.41	30		
Er^{3+} in $LaCl_3$	234	98	0.42	30		
PaF_6^{2-}	2866	1230	0.43	73–76		
$PaCl_6^{2-}$	1264	654	0.52	73–76		
$PaBr_6^{2-}$	976	683	0.70	73–76		
PaI_6^{2-}	725	618	0.85	73–76		
UF_6^{2-}	4337	1792	0.41	73–76		
UCl_6^{2-}	2273	1174	0.52	73–76		
UBr_6^{2-}	1775	1174	0.66	73–76		
$CoCl_4^{2-}$	3600 (5310)	900 (2240)	0.25 (0.42)	81	2.252	82
$CoCl_4^{2-}$	5700	2425	0.42	83		
$CuCl_4^{2-}$	6800	1800	0.26	81	2.23	84
$CoL_N^+Cl_3$	3500	1100	0.30	85		
$NiL_N^+Cl_3$	3250	1000	0.39	85	2.24	86
$Co(Ph_3P)_2Cl_2$	3500	2000	0.57	87		
$Ni(Ph_3P)_2Cl_2$	4500	2000	0.44	87	2.21	88
$Co(Ph_3PO)_2Cl_2$	5700	2425	0.42	89		90
$Ni(POP)Cl_2$	3600	1500	0.41	91		92
$Cu(semicarb)_2Cl_2$	4000	0	0	93	2.85	94
$CoBr_4^-$	3100	775	0.25	81		95
$CuBr_4^-$	5500	850	0.16	81	2.37	96
$CoL_N^+Br_3$	3500	1000	0.28	85		
$NiL_N^+Br_3$	3000	800	0.27	85	2.38	86
$CoBr_3quin^-$	3000 ± 300	450 ± 50	0.15	97–99		
$NiBr_3quin^-$	4500 ± 300	1100	0.23	97–99	2.375	100
$Ni(Ph_3P)Br_3^-$	3000	700	0.23	101	2.37	102
$Co(Ph_3P)_2Br_2$	3500	1500	0.42			
$Ni(Ph_3P)_2Br_2$	4000	1500	0.37	87	2.34	107
$Ni(N{=}C)Br_2$	3500	800	0.22	91	2.35	103
$Ni(biquin)_2Br_2$	3500	850	0.32	91	2.34	104
$Ni(Ph_3P)I_3^-$	2000	600	0.3	91	2.55	105
$Ni(POOP)I_2$	2500	500	0.2	91	2.50	106

[a] In cm^{-1}; X = halogens. [b] In Å.

In principle, the less ambiguous results should be achieved for octahedral complexes of *f* metal ions, since the *f* orbitals are split by the cubic field into three levels, so that the two parameters, e_σ and e_π, can be meaningfully obtained from analysis of the electronic spectra. The values of the parameters are, as expected, smaller for the lanthanides than for the actinides [72–76] because of the more internal nature of the *f* orbitals for the former. The e_σ values do not show large variations throughout the series and e_π/e_σ is fairly large [30,77–80]. Studies on the actinides permit one to obtain the e_σ and e_π values for four halogens. e_σ decreases in the order F > Cl > Br > I, while the e_π/e_σ ratio follows the reverse order [73–76].

For the transition metal ions the values of the e_σ and e_π parameters are much less well defined and consistent sets of data have been reported for only Co^{2+}, Ni^{2+} and Cu^{2+}. For instance, for $CoCl_4^{2-}$ there are two independent determinations of the AOM parameters: in one case $e_\sigma = 3600$ and $e_\pi = 900$ cm^{-1} [81], while in the other $e_\sigma = 5700$ and $e_\pi = 2425$ cm^{-1} [83]. However, since π contributions are known to have little effect upon the spectral properties of tetrahedral cobalt(II) complexes [46], the discrepancy mainly arises from the e_π/e_σ ratio being somewhat arbitrarily fixed by the authors. For instance, if the data of ref. 81 are recast using the same e_π/e_σ ratio as for ref. [83], e_σ becomes 5310 and e_π becomes 2425 cm^{-1}, making the agreement between the two sets of data much better.

A comparison of the data for the same halogen shows that the e_σ values tend to decrease in the series Cl > Br > I but no clear tendency emerges for the e_π values, owing to the above-mentioned indetermination.

(ii) Ammonia and amines

It is generally assumed that $e_\pi = 0$ for ammonia and saturated amines. Although this is certainly an assumption, which has its origin in the molecular orbital orientation of the AOM, it has been verified a few times [28,29] and used in a large number of cases without any obvious inconvenience.

The data in Table 3 show that for nickel(II) and cobalt(II) complexes the e_σ values range from 3700 to 4200 cm^{-1}, as expected on the basis of the relation $10Dq = 3e_\sigma$. There is the exception of the $NiL_N^+X_3$ complexes (X = Cl, Br) for which e_σ values as high as 5900 and 6100 cm^{-1} are reported [85]. Since these values would correspond to $Dq = 1800$ cm^{-1} they seem definitely to be too high. It is suspected that dynamic Jahn–Teller distortions expected for pseudotetrahedral nickel(II) complexes affect the spectra to some extent, thus making the values obtained unreliable.

The amount of data available is not enough to permit an evaluation of the dependence of the e_σ parameter on the number of *R* groups present around

TABLE 3

Angular overlap and structural parameters for ammonia and amine complexes

Compound		e_σ^N [a]	Ref.	Metal–ligand distance [b]	Ref.
$Cr(NH_3)_5OH^{2+}$		7180	108	–	–
$Cr(NH_3)_4Cl_2^+$		7033	109	–	–
$Cr(NH_3)_4Br_2^+$		7220	109	–	–
$Cren_2Cl_2^+ClO_4$		7500	110	–	–
$Cren_2Cl_2^+Cl$		7330	111	–	–
$Cren_2(OH_2)_2^{3+}Cl \cdot H_2O$		7833	110	–	–
		6640	111	–	–
$Crpd_2Cl_2^{2+}$		7400	110	–	–
$Co(en)_3(NO_3)_2$		3700	112	2.13	113
$Co(s\text{-}Et_2en)_2Cl_2$		4065	114	–	–
$CoL_N^+Cl_3$		4250	85	2.09	86
$CoL_N^+Br_3$		4000	85	2.13	86
$CoMe_6trenBr\ Br$		ax 3800		2.15	
		eq 4200	115	2.08	116
$CoNP_3BrPF_6$		900	115	2.76	117
$CoNS_3BrPF_6$		3100	115	2.26	118
$Co(MeTPyEA)(BPh_4)_2$		3800	119	–	120
$Co(MeTPMA)H_2O(ClO_4)_2$		3110	121		121
$Nien_3(NO_3)_2$		3883	122	2.12	123
$Nien_2(NCS)_2$		4010	124	2.09	125
$Ni(NH_3)_4(NCS)_2$		3583	124	2.15	126
$Ni(NH_3)_6Cl_2$		3666	127	2.14	127
$Ni(s\text{-}Et_2en)_2Cl_2$		3972	174	–	–
$Ni(s\text{-}Et_2en)_2Br_2$		3923	128	–	–
$NiL_N^+Cl_3$		6100	85	2.04	86
$NiL_N^+Br_3$		5900	85	2.00	86
$Ni(TMC)N_3^-ClO_4$		4000	129	2.10	130
$Ni(as\text{-}Et_2en)_2(NCS)_2$	NH_2	4650	131	2.08	131
	NEt_2	2485	131	2.30	131
$Ni(as\text{-}Et_2en)_2(H_2O)^{2+}$	NH_2	4770	131	–	–
	NEt_2	2640	131	–	–
$Ni(as\text{-}Me_2en)_2(ONO)_2$	NH_2	4665	132	2.08	133
	NMe_2	3005	132	2.22	133
$Ni(as\text{-}Me_2en)_2(TCA)_2$	NH_2	4545	134	–	–
	NMe_2	3555	134	–	–
$Ni(TMen)_2(NCS)_2$	NMe_2	3165	131	–	–
$Ni(s\text{-}Et_2en)_2(ONO)_2$	NHEt	4490	135	2.12	136

[a] In cm^{-1}. [b] In Å.

the nitrogen donor, i.e. on the nature of the amine. In fact, it must be considered that the metal–nitrogen distance can also be a relevant parameter in determining the value of e_σ. An attempt to establish such a dependence was made in the case of nickel(II) complexes [124] and a smooth increase of e_σ on decreasing the metal–nitrogen distance was found, as expected on the basis of overlap considerations. This series has recently been enlarged [13], confirming the smooth decrease of e_σ on increasing the metal–nitrogen distance.

(iii) Pyridine and aromatic amines

The metal–nitrogen bond involving an aromatic amine, such as pyridine or pyrazole, is characterized by an anisotropic π interaction perpendicular to the aromatic plane. The AOM takes into account this behaviour by putting $e_{\pi\parallel} = 0$ and $e_{\pi\perp} \neq 0$, where $\parallel$ and $\perp$ refer to directions parallel and perpendicular to the aromatic plane, respectively. AO parameters for selected complexes with aromatic amines are reported in Table 4.

For chromium(III) tetrapyridine complexes, $Cr(py)_4A_2$, the four observed electronic transitions did not allow the authors to determine uniquely the five parameters e_σ^A, e_π^A, e_σ^{py}, e_π^{py} and ψ, the angle made by the pyridine plane and the tetragonal plane. In fact two alternative fits were suggested, in which py can act as either a π donor or a π acceptor [109,114,137,138].

The magnetic properties of tetragonal octahedral cobalt(II) complexes CoL_4A_2 depend, neglecting spin–orbit coupling, on the ligand field splitting of the ground state ${}^4T_{1g}(O_h)$ into ${}^4A_{2g}(D_{4h})$ and ${}^4E_g(D_{4h})$, the energy separation $\Delta = E({}^4A_{2g}) - E({}^4E_g)$ being $2(e_\pi^A - e_\pi^L)$ [144]. This fact and the fact that only four electronic transitions are observed, did not permit the precise determination of e_π^L for $Co(py)_4X_2$ ($X = Cl$, Br) and $Co(pz)_4Cl_2$ [144]. The parameters for py in $Co(py)_4X_2$ reported in Table 5 have been transferred from $Fe(py)_4Cl_2$ [146], while the parameters reported in ref. 144 for $Co(py)_4Cl_2$ and $Co(pz)_4Cl_2$ are defined assuming $e_\pi^{Cl} = 0$, and represent the maximum value for $e_{\pi\perp}$,e_π^{Cl} different from zero reducing these values.

The σ bonding ability of the monodentate aromatic amines reported in Table 5 is roughly constant through the series Fe(II), Co(II), Ni(II), while it increases on passing to chromium(III). π-Bonding interactions are always small and positive, the exceptions being $[Ni(quin)Br_3]$ [97], $[Co(quin)Br_3]^-$ [97], and $Ni(biquin)Br_2$ [156]. It must be recalled, however, that a different set of values has been proposed for $[Co(quin)Br_3]^-$ [99] according to which $e_{\pi\perp}$ is positive.

On going to bi- and polydentate amines, both σ and π interactions become stronger and the e_π/e_σ ratio increases. This behaviour reflects the ability of such ligands to stabilize lower oxidation states.

TABLE 4

Angular overlap and structural parameters for pyridine and aromatic amine complexes

Compound	e_{σ}^{N} [a]	$e_{\pi\perp}^{N}$ [a,b]	$e_{\pi\perp}^{N}/e_{\sigma}^{N}$	Ref.	Metal–ligand distance	Ref.
$Fe(py)_4(NCS)_2$	3700	100	0.03	139	2.24	140
$FeDAPSC(ClH_2O)Cl \cdot 2\,H_2O$	4400	200	0.04	141	2.22	142
$CoDAPSC(ClH_2O)Cl \cdot 2\,H_2O$	4500	200	0.04	143	2.19	142
$CoDAPSC(H_2O)_2(NO_3)_2H_2O$	4500	200	0.04	143	2.19	143
$Co(py)_4(NCS_2)$	3700	100–125	0.03	139	–	–
$Co(py)_4Cl_2$	4333	125	0.03	144	2.24	145
$Co(py)_4Cl_2$	3700	100	0.03	146	2.24	145
$Co(py)_4Br_2$	3700	100	0.03	146	–	–
$Co(acac)_2py_2$	3700	400– –200	0.11– –0.05	146	2.18	147, 148
$Co(pz)_4Cl_2$	< 4333	< 250	0.06	144	2.09	149
$Co(iz)_6(NO_3)_2$	3650	353	0.01	150, 151	2.13	152
$Co(NMe\text{-}iz)_6(NO_3)_2$	3390	85	0.02	150, 151	2.12	153
$NiDAPSC(H_2O)_2(NO_3)_2H_2O$	4800	200	0.04	141	2.06	141
$Co(bipy)_3Br_2$	4300	575	0.13	150	2.1	154
$Co(quin)Br_3^-$	3500	−500	0.14	97	–	
	3214	322	–	99		
$Co(tdmmb)(H_2O)_2(BF_4)_2$	5000	1000	0.20	155	2.11	102
$Ni(quin)Br_3^-$	4000	−500	0.13	97	2.029	100
$Ni(biquin)Br_2$	4200	−1000	0.24	156	–	–
$Ni(tdmmb)(H_2O)_2(BF_4)_2$	6000–6500	1000–1500	0.23–0.17	155	2.09	102
$Co(MeTPMA)H_2O(ClO_4)_2$	4550	355	–	121	2.02	121
$Co(MeTPyEA)(BPh_4)_2$	5500	500	–	119	1.94	120
$Cr(py)_4Cl_2$	5700	−720	−0.13	109, 114	–	–
	6767	225	0.03	137		–
$Cr(py)_4Br_2$	5800	−700	−0.12	109, 138	–	–
	6333	−125	−0.02	137	–	–

[a] In cm^{-1}. [b] Refers to the π interaction orthogonal to the aromatic plane. [c] In Å.

(iv) Water

The π interaction is generally assumed to be due to two components, one in the molecular plane ($e_{\pi\|}$) and the other orthogonal to it ($e_{\pi\perp}$). On the reasonable assumption of a strong contribution of in-plane orbitals to σ bond formation, $e_{\pi\perp} > e_{\pi\|}$ seems to make better chemical sense.

For a series of high-spin cobalt(II) complexes, e_σ has been found in the range 2900–3400 cm^{-1} [150,155,121,158], with $e_{\pi\perp}$ fairly small and never exceeding 480 cm^{-1}. An exception is $Co(DAPSC)(H_2O)_2$ [143] for which a much higher e_σ value has been reported. Although the metal–oxygen distance is not shorter than in the other cases [143,102,121,157,159], it should be noted that for the higher e_σ value the corresponding Dq value for $Co(DAPSC)(H_2O)_2$ would be 1190 cm^{-1}, which is definitely higher than the value generally accepted for water in high-spin cobalt(II) complexes [166]. A similar consideration holds for the corresponding nickel(II) complexes [141], for which the Dq value would be 1360 cm^{-1}. The values reported for the copper complexes are different from each other [162,164] and also from the values reported for the other metal ions, and must reflect the well-known difficulty in obtaining a consistent set of ligand field parameters for copper(II) complexes.

(v) R-Oxide (R = N, P, As)

The e_λ parameters for the R-oxide molecules (R = N, P, As) are shown in Table 6. The e_σ and e_π parameters have the same sign, independently of the

TABLE 5

Angular overlap and structural parameters for water complexes

Compound	$e_\sigma^{OH_2}$ [a]	$e_{\pi\perp}^{OH_2}$ [a,b]	$e_{\pi\|}^{OH_2}$ [a,b]	Ref.	Metal–ligand distance [c]	Ref.
$Co(H_2O)_6^{2+}$	2920	110	60	144	2.146	152
$Co(acac)_2(H_2O)_2$	3220	480	190	152	2.148	153
$Co(MeTPyEA)H_2O^{2+}$	3400	204	102	102	2.02	102
$Co(3MeOSALen)H_2O$	4863	1247		154	2.12	155
$Co(tdmmb)(H_2O)_2(BF_4)_2$	3500	1000		149	2.18	102
$Co(DAPSC)(H_2O)_2^{2+}$	4500	400		137	2.146	137
$Ni(tdmmb)(H_2O)_2(BF_4)_2$	3800	1300		149	2.09	102
$Ni(DAPSC)(H_2O)_2^{2+}$	5200	500		135	2.069	135
$Cu(phen)_2H_2O$	2100	40	10	156	2.181	157
$Cu(H_2O)_6^{2+}$	4520	1450	1530	158	2.089	159

[a] In cm^{-1}. [b] $\perp$ and $\|$ refer to the π interaction orthogonal and parallel to the water molecule plane. [c] In Å.

nature of the atom bound to oxygen in the ligand molecule and of the geometry of the complexes; in general, however, agreement between the different sets of parameters is far from satisfactory. Note that the Dq values on which the electronic spectra depend are identical for the two sets of parameters. For high-spin octahedral cobalt(II) complexes the magnetic properties are not very sensitive to the e_π/e_σ ratio, but only to the difference in π bonding abilities [46]. Since, in general, the M–O moiety does not possess cylindrical symmetry, the π interactions are expected to be anisotropic, as is confirmed by the majority of the compounds examined. In fact, the largely anisotropic paramagnetic and spectral properties of octahedral pyridine-*N*-oxide metal(II) complexes (metal = Co, Ni, Mn) could be explained easily only within the AOM [167,173], while ligand field models, which assume metal–ligand interactions of cylindrical symmetry, could not explain them at all. In these complexes the anisotropic π interaction is generally assumed to have one component normal and one parallel to the M–O–R plane. The ratio between the two interactions has often been fixed close to two, on the assumption of an sp^2 hybridized oxygen atom [167,177].

(vi) Schiff bases derived from salicylaldehyde and acetylacetone

The oxygen and nitrogen donor atoms of Schiff bases derived from salicylaldehyde and acetylacetone are assumed to have different π interactions with the metal ion. The oxygen atom has different π interactions, assumed to be parallel and perpendicular to the salicyl ring, while the

TABLE 6

Angular overlap and structural parameters for R-oxide complexes (R=N, P, As)

Compound		$e_\sigma^{0\ a}$	$e_\pi^{0\ a,b}$	$e_\pi^{0\ a,b}$	e_π^0/e_σ^0	Ref.	Metal–ligand distance [c]	Ref.
$Co(PyNO)_6^{2+}$		4300	1330	665	0.464	161	2.088	162
$Co(PyNO)_6^{2+}$		3575	608	304	0.255	144	2.088	162
$Co(apy)_6^{2+}$		2680	202	93	0.110	144	2.446	163
$Co(picNO)_5(ClO_4)_2$	ax	4725	1185		0.251	164	2.081	165
	ea	5250	1315		0.251		1.984	
$Co(Ph_3PO)_2Cl_2$		4750	1945	1555	0.737	89	1.999	90
$Co(MePh_2AsO)_4NO_3(NO_3)$		6685	2765		0.414	61	2.00	59
$Ni(PyNO)_6^{2+}$		4393	1660	830	0.657	166	2.088	165

[a] In cm^{-1}. [b] x and y refer to the π interaction orthogonal and parallel to the M–O–R plane, respectively. [c] In Å.

TABLE 7

Angular overlap and structural parameters of Schiff base derived from salicylaldehyde and acetylacetone complexes [a]

Compound	e_σ^N	e_π	e_π	e_σ/e_π	Ref.	Metal–ligand distance [c]	Ref.
5 ClNi(SALNdiethyl)	3300	0	900	0.273	176	1.98	177
	4400 (e_σ^0)	900	1300	0.5		1.94 (R_{M-O})	
Ni(SALNisopropyl)	3800	0	930	0.245	2,178	1.970	184
	4200 (e_σ^0)	1000	660	0.395		1.896	
Co(SALNisopropyl)	5000	not considered			167	1.970	168
	5000	not considered				1.896	
Ci(SALNmethyl)	3345	0	270	0.081	169		170
	4100	190	545	0.180			
Co(SALen)	5833	2018	3315	0.914	154–171	1.849	172
Co(SALen)dimer	5215	1646	2705	0.834	154–171	1.908	173
Co(SALen)py	5275	1669	2742	0.834	154–171	1.90	174
Co(3MeOSALen)H_2O	4273	1102	1810	0.682	154–171	2.00	155
Cu(acacen)	4600	1400	2300	0.804	154–171	1.94	175

[a] All the $e\lambda$ parameters are in cm^{-1}. [b] ∥ and ⊥ indicate the π interaction in the metal–donor–R plane and normal to it, respectively. [c] In Å.

nitrogen donor, which can be considered to be sp^2 hybridized, only has an interaction perpendicular to the M–N=C plane, where C is the carbon atom of the carboxyl group. This hypothesis is confirmed by experiment and the e_π parameters obtained for different high-spin nickel and cobalt(II) complexes compare well with each other (Table 7). In CoSALNisopropyl the possibility of a π interaction was not taken into consideration, so as to have the minimum number of parameters, therefore different e_σ value are reported in this case [177].

Larger e_σ and e_π values were reported for low-spin cobalt(II) complexes [160,177]. Although in this case the analysis was very approximate, the increase in the e_λ parameters on going from high- to low-spin cobalt(II) complexes appears to be quite reasonable.

(vii) Acetylacetonate

The data reported in the literature (Table 8) are insufficient for a definite trend to be seen in the bonding ability of the oxygen donors in the acetylacetonate ligand. Further, most of the reported data refer to high-spin octahedral cobalt(II) complexes, whose magnetic properties depend on a factor $\Delta = 4e_\pi^{\mathrm{acac}} - 2e_\pi^{\mathrm{acac}} - 2e_\pi$ axial (|| and ⊥ refer to the in-plane and out-of-plane π interaction with the acetylacetonate moiety). Therefore, for a given axial ligand it is possible to obtain, to a first approximation, only the difference between the two e_π parameters and not the absolute values. Nevertheless, the experimental evidence allows us to deduce that the out-of-plane π interaction, associated with the π bond delocalized over the chelating ring of the acetylacetonate ligand, is generally stronger than the in-plane one.

TABLE 8

Angular overlap and structural parameters for acetylacetonate complexes

Compound	e_σ^{0} [a]	$e_{\pi\perp}^{0}$ [a,b]	$e_{\pi\parallel}^{0}$ [a,b]	Ref.	Metal–ligand distance [c]	Ref.
$Co(acac)_2(H_2O)_2$	4890	1010	820	152	2.035	153
$Co(acac)_2(6Mequin)_2$	4820	980	750	152	2.036	179
$Co(acac)_2(py)_2$	3500	$e_{\pi\perp} > e_{\pi\parallel}$	$e_{\pi\perp} > e_{\pi\parallel}$	140	2.034	142
$Cu(acac)_2(quin)_2$	7500	2250	1725	180		

[a] In cm^{-1}. [b] ⊥ and || refer to the π interactions orthogonal and parallel to the acetylacetonate plane. [c] In Å.

(viii) Phosphines

The e_λ parameters for the phosphine ligands are shown in Table 9. Compared to the other sets of ligands reported here so far, all the phosphines have negative e_π values, requiring a substantial metal–ligand bonding interaction, rather than an antibonding one. The e_σ and e_π values are rather similar in the series of high-spin cobalt(II) complexes [87,115]. Much larger e_σ and e_π/e_σ values were reported for a low-spin cobalt(II) complex [192]. These parameters are also larger in the nickel(II) series of complexes [87,91,101], compared to the series of high-spin cobalt(II) complexes. In fact, *Dq* values as high as 2400 cm^{-1} are required by the AOM parameters used for $[Ph_4As]Ni(PPh_3)I_3$ [91]. Again, since these complexes are pseudotetrahedral, it is possible that dynamic Jahn–Teller effects may invalidate the description of the coordination environment on the basis of the X-ray crystal structure. Similar considerations hold for the nickel(I) complex, Nip_3Cl [189], which is also expected to have a degenerate ground state.

(ix) Bio-inorganic applications

Recently, Solomon and co-workers reported a crystal field analysis of the single-crystal electronic and EPR spectra of plastocyanin [191], a so-called blue copper protein. The X-ray structure determination of plastocyanin from *Populus nigra* showed that copper is co-ordinated to two nitrogen atoms of two histidines, a sulphur of a cysteine and a sulphur of a methionine [192].

The analysis of the electronic and EPR spectra of plastocyanin is difficult,

TABLE 9

Angular overlap and structural parameters of phosphine ligands

Compound	$e_\sigma^{P\,a}$	$e_\pi^{P\,a}$	e_π^P/e_σ^P	Ref.	Metal–ligand distance [b]	Ref.
$Co(PPh_3)_2Cl_2$	4000	−1000	0.25	87	2.31	88
$Co(PPh_3)_2Br_2$	3500	−1000	0.29	87	2.32	88
$Co(NP_3)BrPF_6$	3680	−830	0.23	175	–	117
$Co(PEt_2P)_2mes_2$	6000	−4300	0.57	181	1.23	182
$Ni(PPh_3)_2Cl_2$	4500	−2500	0.56	87	2.31	88
$Ni(PPh_3)_2Br_2$	4000	−1500	0.38	87	2.32	88
$Ni(PPh_3)Br_3Ph_4As$	5000	−1500	0.30	101	2.32	102
$Ni(PPh_3)I_3Ph_4As$	6000	−1500	0.25	97	2.28	105
$NiPOPCl_2$	5000	−1500	0.30	97	2.31	92
Nip_3Cl	5000	−1000	0.20	183	2.22	184

[a] In cm^{-1}. [b] In Å.

since the crystal structure is known only to a low accuracy [192]. Another point which must be made is that the crystal field (and AOM) analysis of simple copper(II) complexes is often not fully successful [193,194], and several sophistications have been included in the model in order to fit the energies of the electronic transitions [195]. Therefore the values which are obtained for the parameters should be regarded with even more caution than is usually needed for other metal ions. However, the crystal field analysis of Solomon and co-workers [191] was indeed successful in describing at least the nature of the ground state. This induced us to perform a similar analysis with the AOM to check whether or not reasonable results could be obtained employing parameters which do not contradict those usually found for simple complexes.

To analyse the spectra of the metallo-protein, Solomon and co-workers obtained the parameters from reported data for simple copper(II) complexes, namely $Cu(iz)_4(NO_3)_2$ [191] and $Cu(iz)_6(ClO_4)_2$ [197]. In the crystal field approach the metal–ligand interaction is assumed to be isotropic, but this seems hardly to be the case for the imidazole ligand, as was shown in Section (iii) for other aromatic amines. On translating the values of the parameters used by Solomon into the AOM language we find, for example, for a nitrogen atom at 2.01 Å from the copper ion, $e_\sigma^N = 9876$ cm^{-1}, $e_\pi^N = 4214$ cm^{-1}. Comparing these values with those reported in Table 4 for similar ligands, we find that both e_σ and e_π are much higher than usual.

The energies of the electronic transitions for $Cu(iz)_4(NO_3)_2$, where the four Cu–N bond distances are extremely similar to each other [196] (2.008, 2.009, 2.010 and 2.018 Å, respectively) and the imidazole planes are practically orthogonal to the equatorial plane, can be fitted using only two parameters, e_σ^N and $e_{\pi\perp}^N$, for the imidazole ligands, $e_{\pi\perp}$ being the interaction orthogonal to the aromatic plane. Since the complex also has an axial nitrate at 2.60 Å, one should also include e_σ^0 and e_π^0 parameters, but, due to the long metal–oxygen distance it is assumed that the e_π interaction is zero. Within the assumed tetragonal symmetry, the energies of the transitions from the ground x^2-y^2 state are given by

$$\begin{aligned}\Delta(xy) &= 3e_\sigma^N - 4e_{\pi\perp}^N \\ \Delta(z^2) &= 2e_\sigma^N - 2e_\sigma^{ax} \qquad (22) \\ \Delta(xz, yz) &= 3e_\sigma^N\end{aligned}$$

Two different assignments have been reported in the literature [196] for $Cu(iz)_4(NO_3)_2$: in one case the $\Delta(xy)$ and $\Delta(z^2)$ transitions have been located at 15400 and 12500 cm^{-1}, respectively, while in the other assignment the two transitions were reversed. The highest frequency band at 18800 cm^{-1} has been assigned to the $\Delta(xz, yz)$ transition in both cases. The calculated parameters for the first assignment are: $e_\sigma^{\mathrm{N}} = 6270\ \mathrm{cm}^{-1}$, $e_{\pi\perp}^{\mathrm{N}} = 850\ \mathrm{cm}^{-1}$, $e_\sigma^{0} = 10\ \mathrm{cm}^{-1}$, while for the second they are: $e_\sigma^{\mathrm{N}} = 6270\ \mathrm{cm}^{-1}$, $e_{\pi\perp}^{\mathrm{N}} = 1575\ \mathrm{cm}^{-1}$, $e_\sigma^{0} = -1430\ \mathrm{cm}^{-1}$. Of the two sets of parameters the first definitely seems more acceptable, with a small e_σ^0, as expected for the long Cu–O distance, while the second yields an improbable negative e_σ^0 value. The difference between our calculated values and those given by Solomon and co-workers [191], $e_\sigma^{\mathrm{N}} = 9786$, $e_\pi^{\mathrm{N}} = 4214\ \mathrm{cm}^{-1}$, is understood if one expresses the energies of the transitions in terms of isotropic π interaction. In this case we find

$$\begin{aligned} \Delta(xy) &= 3e_\sigma^{\mathrm{N}} - 4e_\pi^{\mathrm{N}} \\ \Delta(z^2) &= 2e_\sigma^{\mathrm{N}} - 2e_\sigma^{\mathrm{ax}} \\ \Delta(xz, yz) &= 3e_\sigma^{\mathrm{N}} - 2e_\pi^{\mathrm{N}} \end{aligned} \qquad (23)$$

It is apparent that, for positive e_π^{N} values, e_σ^{N} must be higher than when we use eqn. (22).

If now we analyse the spectra of $\mathrm{Cu(iz)_6(NO_3)_2}$ [190], we see that, of the four equatorial imidazole ligands, two are at a distance of 2.012 Å from the copper, and two are at 2.049 Å. In this case the angles the imidazole rings make with the equatorial plane are significantly different from 90 °, i.e., 70° and 35 ° for each set of imidazoles, respectively [190]. Also in this case the axial imidazoles are at a much longer distance, 2.59 Å.

A fit of the observed transitions was attempted by keeping the $e_\sigma^{\mathrm{N_1}}$ and $e_{\pi\perp}^{\mathrm{N_1}}$ parameters of the nitrogen at 2.012 Å, $\mathrm{N_1}$, fixed at the value obtained for $\mathrm{Cu(iz)_4(NO_3)_2}$, and varying $e_\sigma^{\mathrm{N_2}}$ and $e_{\pi\perp}^{\mathrm{N_2}}$ for the nitrogen at 2.049 Å, $\mathrm{N_2}$, and only $e_\sigma^{\mathrm{N_3}}$ for that at 2.59 Å, $\mathrm{N_3}$. The $e_\sigma^{\mathrm{N_2}}$ value is determined by the energy of the highest transition $\Delta(xz, yz)$, at $4500 \pm 500\ \mathrm{cm}^{-1}$, while $e_{\pi\perp}^{\mathrm{N_2}}$ is less easily fixed, since the energy of the $\Delta(xy)$ transition is determined experimentally with only a limited accuracy. In this case two assignments were also proposed [193], but we prefer that which sets $\Delta(z^2)$ at the lowest energy, by analogy with $\mathrm{Cu(iz)_4(NO_3)_2}$. In fact in all our calculations we found it extremely difficult to put $\Delta(xy)$ at a much lower energy than $\Delta(xz, yz)$. A reasonable fit was obtained with $e_\sigma^{\mathrm{N_2}} = 4270$, $e_{\pi\perp}^{\mathrm{N_2}} = 750$ and $e_\sigma^{\mathrm{N_3}} = 200\ \mathrm{cm}^{-1}$, with the calculated transitions (observed transitions shown in parentheses) at 10700 (10700), 13621 (12500), 15354 and 16087 (16200 cm^{-1}. As can be seen the agreement is far from good for the Δxy transition (13621 versus 12500) but a small error in the experimental determination yields a large uncertainty in the parameters. Therefore it does not seem to be realistic to use fixed values of parameters and transfer them simply from one chromophore to another, since they are affected in any case by a consistent error.

The situation of course becomes even more complicated when one tries to fit the spectral properties of metallo-enzymes. In general, the uncertainty of the structural parameters within the coordination polyhedron is much larger than is found in simple model complexes, and the energies of the electronic transitions are often determined with lower accuracy. Following Solomon and co-workers [191] we tried to reproduce the energies of the electronic transitions for plastocyanin using the different parameters calculated for the model complexes.

To reduce the number of parameters to a minimum we fixed e_σ and $e_{\pi\perp}$ for the two nitrogen donors at the value found for $\mathrm{Cu(iz)_4(NO_3)_2}$ and varied the e_σ and e_π parameters for the two sulphur donors. Since the copper–methioninsulphur distance is as long as 2.90 Å [192] we expected e_σ^{Sme} to be small, presumably very close to zero. Therefore in this approximation the energies are determined mainly by the parameters for the cysteine sulphur. The fits obtained are not excellent but, because of uncertainties associated with the electronic transition and the structural parameters, they can be considered satisfactory. The values required are: $e_\sigma^{\mathrm{Scy}} = 4000 \pm 1000$ $\mathrm{cm^{-1}}$, $e_\pi^{\mathrm{Cys}} = 1500 \pm 500$ $\mathrm{cm^{-1}}$ and $e_\sigma^{\mathrm{Sme}} = 500 \pm 500$ $\mathrm{cm^{-1}}$, yielding transition energies at 4500 ± 700 $\mathrm{cm^{-1}}$, 7000 ± 500 $\mathrm{cm^{-1}}$, 9200 ± 300 $\mathrm{cm^{-1}}$ and $10\,000 \pm 300$ $\mathrm{cm^{-1}}$, compared with the experimental values of 5000, 9150 and 11 200 $\mathrm{cm^{-1}}$. It is satisfactory that the nature of the ground state remains substantially constant in the above range of parameters. In fact, the ground state orbital is essentially localized orthogonal to the Cu–methionine bond, as was found by Solomon and co-workers, and in agreement with their finding that the largest g value is closely parallel to this bond direction [191].

An interesting application of single-crystal EPR spectroscopy to the description of low-spin ferric porphyrin complexes has recently been reported by Strouse and co-workers [198]. Although they did not use the AOM, their results are easily described within this framework.

Octahedral low-spin iron(III) has a ground t_{2g}^5 configuration, which for most purposes can be used to describe the ground state. Low-symmetry effects determine the splitting of the three t_{2g} orbitals, but, as long as the complexes remain orthoaxial, i.e. the bond angles are those of a regular

TABLE 10

Angular overlap matrix for octahedral low-spin iron(III) porphyrins

$\lvert yz\rangle$	$\lvert xz\rangle$	$\lvert xy\rangle$
$\langle yz \rvert 2e^{\mathrm{N}}_{\pi\perp} + \sum_{i=1}^{2} (\cos^2_{\Psi i} e^i_{\pi y} + \sin^2_{\Psi i} e^i_{\pi x})$	$\sum_{i=1}^{2} \sin_{\Psi i} \cos_{\Psi i} (e^i_{\pi y} - e^i_{\pi x})$	0
$\langle xz \rvert$	$2e^{\mathrm{N}}_{\pi\perp} + \sum_{i=1}^{2} (\sin^2_{\Psi i} e^i_{\pi y} + \cos^2_{\Psi i} e^i_{\pi x})$	0
$\langle xy \rvert$		$4e^{\mathrm{N}}_{\pi\parallel}$

octahedron, the *xz*, *yz*, and *xy* orbitals are π bonding. Since this is almost always the case for the iron porphyrins, the AOM yields for these three orbitals the matrix shown in Table 10. $e_{\pi\|}^{\mathrm{N}}$ and $e_{\pi\perp}^{\mathrm{N}}$ represent the π interactions parallel and orthogonal to the equatorial plane, respectively; $e_{\pi y}^{i}$ and $e_{\pi x}^{i}$ are the π interactions of the i axial ligand, parallel to the y and x directions, respectively, as defined in Fig. 2. ψ_i is the angle between the x axis for ligand i and the x axis of the frame centred on the metal. The matrix in Table 10 shows that the *yz* and *xz* orbitals can be admixed if the axial ligands are not linearly ligating, i.e. if $e_{\pi y}^{i} \neq e_{\pi x}^{i}$. The energies of the orbitals are given by

$$\begin{aligned}
E(x'y') &= 4e_{\pi\|}^{\mathrm{N}}\\
E(y'z') &= 2e_{\pi\perp}^{\mathrm{N}} + \tfrac{1}{2}\sum_i \left(e_{\pi y}^{i} + e_{\pi x}^{i}\right)\\
&\quad + \tfrac{1}{2}\left[\sum_i \cos 2_{\psi_i}\left(e_{\pi y}^{i} + e_{\pi x}^{i}\right)^2 + \sum_i \sin 2_{\psi_i}\left(e_{\pi y}^{i} + e_{\pi x}^{i}\right)\right]^{1/2} \qquad (24)\\
E(x'z') &= 2e_{\pi\perp}^{\mathrm{N}} + \tfrac{1}{2}\sum_i \left(e_{\pi y}^{i} + e_{\pi x}^{i}\right)\\
&\quad - \tfrac{1}{2}\left[\sum_i \cos 2_{\psi_i}\left(e_{\pi y}^{i} + e_{\pi x}^{i}\right)^2 + \sum_i \sin 2_{\psi_i}\left(e_{\pi y}^{i} + e_{\pi x}^{i}\right)\right]^{1/2}
\end{aligned}$$

$y'z'$ and $x'z'$ are linear combinations of the *xz* and *yz* orbitals according to

$$\begin{aligned}
|y'z'\rangle &= \cos\alpha\,|yz\rangle + \sin\alpha\,|xz\rangle\\
|x'z'\rangle &= \sin\alpha\,|yz\rangle - \cos\alpha\,|xz\rangle
\end{aligned} \qquad (25)$$

where

$$\alpha = \tfrac{1}{2}\tan^{-1}\frac{\sum_i \sin 2\psi_i\left(e_{\pi y}^{i} - e_{\pi x}^{i}\right)}{\sum_i \cos 2\psi_i\left(e_{\pi y}^{i} - e_{\pi x}^{i}\right)} \qquad (26)$$

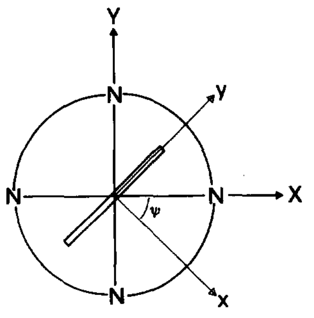

Fig. 2. Metal centred and axial ligand centred coordinate frames.

In the literature it is customary to express the energies of the $^2T_{2g}$ manifold by two parameters, V and Δ [199], as defined in Fig. 3, which in the AOM formalism are

$$\begin{aligned} V &= \left\{ \left[\sum_i \cos 2\psi_i \left(e^i_{\pi y} - e^i_{\pi x} \right) \right]^2 + \left[\sum_i \sin 2\psi_i \left(e^i_{\pi y} - e^i_{\pi x} \right) \right]^2 \right\}^{1/2} \\ \Delta &= -4e^{\mathrm{N}}_{\pi\|} + 2e^{\mathrm{N}}_{\pi\perp} + \tfrac{1}{2}\sum_i \left(e^i_{\pi y} + e^i_{\pi x} \right) \end{aligned} \qquad (27)$$

In the case of two identical ligands on the z axis the expressions (27) reduce to those given by Strouse and co-workers [198] provided that

$$\begin{aligned} \pi_{\mathrm{a}} &= e_{\pi y}; \qquad & e^{\mathrm{N}}_{\pi\|} &= \pi'_{\mathrm{p}} \\ \pi'_{\mathrm{a}} &= e_{\pi x}; \qquad & e^{\mathrm{N}}_{\pi\perp} &= \pi_{\mathrm{p}} \end{aligned} \qquad (28)$$

Since the $e^{\mathrm{N}}_{\pi\|}$ interaction is fairly weak, the yz and xz orbitals generally are at higher energy than the xy orbitals and the unpaired electron will be in one of the former orbitals. This pattern can be reversed, however, if the axial ligands are π acceptors rather than π donors.

With the hypothesis that $E(y'z') > E(x'z') > E(x'y')$, the expected g tensor, in a perturbation treatment which can be used as a first approximation, is

$$\begin{array}{ccc} g_e + \dfrac{2}{\Delta_{xy}}\sin^2\alpha & -2\sin\alpha\cos\alpha\dfrac{\lambda}{\Delta_{xy}} & 0 \\ & g_e + \dfrac{2\lambda}{\Delta_{xy}}\cos^2\alpha & 0 \\ & & g_e + \dfrac{2\lambda}{\Delta_{x'y'}} \end{array} \qquad (29)$$

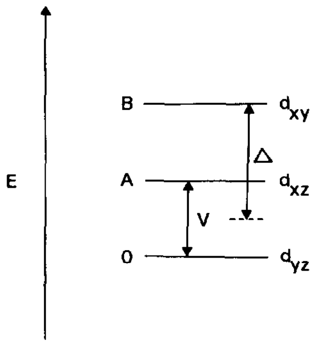

Fig. 3. Energy level diagram for the t_{2g} orbitals, showing the V and Δ parameters.

where $\Delta_{xy} = E(x'y') - E(y'z')$; $\Delta_{xz} = E(x'z') - E(y'z')$, λ is the spin–orbit coupling constant. The **g** tensor is diagonal within a frame with z parallel to Z; $x' = \sin(-\alpha)y - \cos(-\alpha)x$; $y' = \cos(-\alpha)x + \sin(-\alpha)y$, i.e. the same α angle can express the linear combination of both the wavefunctions, as shown in eqn. (25), and the reference frame which diagonalizes the **g** tensor. However, the sign is such that if the wavefunctions rotate by $+\alpha$, **g** rotates by $-\alpha$ [199]. The corresponding principal g values are

$$g_{x'x'} = g_e; \qquad g_{y'y'} = g_e + \frac{2\lambda}{\Delta_{xy}}; \qquad g_{z'z'} = g_e + \frac{2\lambda}{\Delta_{xz}} \tag{30}$$

If there is one axial ligand, or two identical axial ligands, then the π anisotropy determines the orientation of **g** as shown by eqn. (30). This means that the α angle is the angle that the direction of the stronger π interaction of the axial ligand makes with the X reference axis. In fact, in this case eqn. (24) yields $e(y'z') = 2e_{\pi}^{N} + e_{\pi y}$, $E(x'z') = 2e_{\pi}^{N} + e_{\pi x}$, and in our hypothesis of $y'z'$ having the highest energy, $e_{\pi y}$ must be larger than $e_{\pi x}$.

Since λ and Δ_{xy}, Δ_{xz} in eqn. (30) are positive values, $g_{x'x'}$ will be the smallest g value. It was found to make an angle of 90° $+2\alpha$ with the direction of maximum π interaction with the axial ligands.

When the two axial ligands are different, eqn. (26) shows that the α angle is not easily related to the direction of the maximum π interaction, unless one of the two is linearly ligating. Therefore trying to obtain structural information from the direction of the **g** values may be dangerous.

(x) A classic mixed-valence system: the Creutz–Taube cation

A final example of the AOM is the long-debated electronic structure of the Creutz–Taube [200] cation $[(NH_3)_{10}Ru_2pyr]^{5+}$

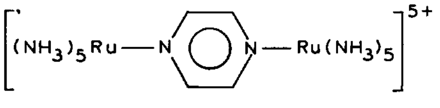

The ion has been described either as class II or class IIIA in the Robin and Day mixed valence classification [201]. Class II means that the Ru^{III} and Ru^{II} valences are trapped, while Class IIIA means that the unpaired electron is in a molecular orbital encompassing both the metal ions.

EPR spectra have been used to advocate both the descriptions. In particular, Burker et al. showed that the EPR spectra of $[(NH_3)_{10}Ru_2pyr]^{5+}$ are practically identical to the spectra of $[(NH_3)_{10}Ru_2pyr]^{6+}$, which contains two identical Ru^{III} ions, and concluded on this basis that the unpaired electron is localized on the Ru^{III} ion in the mixed valence species [202]. On

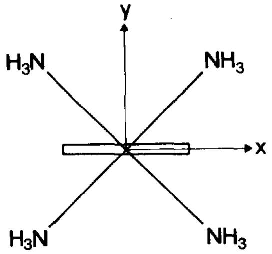

Fig. 4. Coordinate frame for $|(NH_3)_{10}Ru_2pyr|^{5+}$.

the other hand Hush et al. recorded the single-crystal EPR spectra of $[(NH_3)_{10}Ru_2pyr]Br_4Cl$ and found that the orthorhombic g tensor $g_1 = 2.779$, $g_2 = 2.489$, $g_3 = 1.334$ has principal directions such that g_3 is orthogonal to the pyrazine plane and g_1 is parallel to the Ru–pyr bond direction [203]. They analysed the data on the basis of the theory for low-spin d^5 ions and concluded correctly that the unpaired electron must be in a $|yz\rangle$ orbital with the axes defined in Fig. 4.

However, the authors assumed that the unpaired electron can be in the $|yz\rangle$ orbital only if substantial metal–metal interaction is operative, while for a localized Ru(III) the g_3 value should be parallel to the Ru–pyrazine bond direction. Actually what the EPR data indicate is that the Ru–pyrazine interaction is anisotropic and that the order of the levels is determined by the π anisotropy of the pyrazine ligand. It seems, therefore, that no definite conclusion can be reached on the long-debated problem [204].

J. CONCLUSIONS

The AOM is a very useful tool for the calculation of paramagnetic properties of transition metal complexes. Although we are not at the point of transferring rigidly the values of the e_λ parameters from one ligand to another, and presumably we will never arrive at this point, due to the inherent limitations of the model, we believe that it is possible to have a feeling for the range of values that can be expected for a particular ligand with a particular metal ion. It seems therefore that the time is coming to tackle the difficult task of describing the electronic structure of biological systems involving metal ions through the AOM.

ACKNOWLEDGEMENT

Thanks are due to Prof. D.R. McMillan, Purdue University, for helpful discussions on the possible applications of the AOM to bio-inorganic systems.

REFERENCES

1 C.E. Schäffer and C.K. Jørgensen, Mol. Phys., 9 (1965) 401.
2 C.K. Jørgensen, R. Pappalardo and H.H. Schmidtke, J. Chem. Phys., 39 (1963) 1422.
3 C.E. Schäffer, Proc. R. Soc. London, Ser. A, 297 (1967) 96.
4 C.E. Schäffer, Struct. Bonding (Berlin), 5 (1968) 68.
5 C.E. Schäffer, Struct. Bonding (Berlin), 14 (1973) 69.
6 S.E. Harnung and C.E. Schäffer, Struct. Bonding (Berlin), 12 (1972) 201.
7 S.E. Harnung and C.E. Schäffer, Struct. Bonding (Berlin), 12 (1972) 257.
8 C.E. Schäffer, in W.C. Price, S.S. Chissick and T. Ravensdale (Eds.), Wave Mechanics, Butterworths, London, 1973, p. 173.
9 M.R. Kibler, J. Chem. Phys., 55 (1971) 1989.
10 M.R. Kibler, J. Chem. Phys., 61 (1974) 3859.
11 M.R. Kibler, Int. J. Quantum Chem., 9 (1975) 403.
12 M.R. Kibler, Aust. J. Chem., 35 (1982) 231.
13 P.J. Steenkamp and J.W. Gonsalves, Aust. J. Chem., 33 (1980) 1705.
14 D.W. Smith, Struct. Bonding (Berlin), 12 (1972) 49.
15 D.W. Smith, Struct. Bonding (Berlin), 35 (1978) 87.
16 I. Bertini, D. Gatteschi and A. Scozzafava, Isr. J. Chem., 15 (1976/77) 189.
17 A. Bencini and D. Gatteschi, Inorg. Chim. Acta, 31 (1978) 11.
18 R.G. Woolley, Mol. Phys., 42 (1981) 703.
19 A.B.P. Lever and B.R. Hollebone, Inorg. Chem., 11 (1972) 2183.
20 A.B.P. Lever, Coord. Chem. Rev., 43 (1982) 63.
21 M. Gerloch and R.C. Slade, Ligand Field Parameters, Cambridge University Press, London, 1973.
22 C.J. Ballhausen, Introduction to Ligand Field Theory, McGraw-Hill, New York, NY, 1962.
23 R.S. Drago, Physical Methods in Chemistry, W.B. Saunders, Philadelphia, PA, 1977.
24 C.K. Jørgensen, Absorption Spectra and Chemical Bonding in Complexes, Pergamon Press, Oxford, 1962.
25 M. Gerloch and R.F. McMeeking, J. Chem. Soc. Dalton Trans., (1975) 2443.
26 M. Wolfsberg and L.J. Helmholz, J. Chem. Phys., 20 (1952) 837.
27 J. Tennyson and J.R. Murrell, J. Chem. Soc. Dalton Trans., (1980) 2395.
28 C.K. Jørgensen, Modern Aspects of Ligand Field Theory, North-Holland, Amsterdam, 1971.
29 M. Gerloch and R.G. Woolley, J. Chem. Soc. Dalton Trans., (1981) 1714.
30 C. Linares, A. Lonat and M. Blanchard, Chem. Phys., 68 (1982) 453.
31 W. Urland, Chem. Phys., 14 (1976) 393.
32 M. Gerloch, J. Harding and R.G. Woolley, Struct. Bonding (Berlin), 46 (1981) 1.
33 J.C. Slater, The Self Consistent Field for Molecules and Solids. Volume 4. Quantum Theory of Molecules and Solids, McGraw-Hill, New York, NY, 1974.
34 D.W. Smith, Inorg. Chim. Acta, 22 (1977) 107.
35 D.J. Mackey, R.F. McMeeking and M.A. Hitchman, J. Chem. Soc. Dalton Trans., (1979) 299.
36 P. Fantucci and V. Valenti, J. Am. Chem. Soc., 98 (1976) 3832.
37 J.S. Griffith, The Theory of Transition-Metal Ions, Cambridge University Press, London, 1971.
38 A. Bencini and D. Gatteschi, in B.N. Figgis and G.A. Melson (Eds.), Transition Metal Chemistry, Marcel Dekker, New York, NY, 1982, p. 106 and references therein.

39 C.K. Jørgensen, Discuss. Faraday Soc., 26 (1958) 110.
40 Y. Tanabe, Prog. Theor. Phys. Suppl., 14 (1960) 17.
41 K.W.H. Stevens, Proc. R. Soc. London, Ser. A., 219 (1953) 542.
42 W. Low, in F. Seitz and D. Turnbull (Eds.), Paramagnetic Resonance in Solids, Academic Press, New York, NY, 1960.
43 B.J. Hatway and D.E. Billing, Coord. Chem. Rev., 5 (1970) 143.
44 M.H.L. Pryce, Proc. Phys. Soc., Ser. A, 63 (1950) 25.
45 A. Abragam and M.H.L. Pryce, Proc. R. Soc. London, Ser. A, 205 (1951) 137.
46 L. Banci, A. Bencini, C. Benelli, D. Gatteschi and C. Zanchini, Struct. Bonding (Berlin), 52 (1982) 37.
47 J.E. Wertz and J.R. Bolton, Electron Spin Resonance Elementary Theory and Practical Applications, McGraw-Hill, New York, NY, 1972.
48 P.W. Anderson and P.R. Weiss, Rev. Mod. Phys., 25 (1963) 269.
49 A. Abragam and B. Bleany, Electron Paramagnetic Resonance of Transition Metal Ions, Clarendon Press, Oxford, 1970.
50 B.R. McGarvey, Transition Met. Chem., 3 (1966) 89.
51 A. Bencini and D. Gatteschi, J. Am. Chem. Soc., 105 (1983) 5535.
52 B.R. McGarvey, J. Phys. Chem., 71 (1967) 51.
53 A. Bencini and D. Gatteschi, J. Magn. Reson., 34 (1979) 653.
54 A. Blake, J. Chem. Soc. Dalton Trans., (1981) 1041.
55 J.H. Van Vleck, The Theory of Electric and Magnetic Susceptibilities, Oxford University Press, London, 1959.
56 W. DeW. Horrocks and D. DeW. Hall, Coord. Chem. Rev., 6 (1971) 147.
57 S. Mitra, Prog. Inorg. Chem., 22 (1977) 293.
58 M. Gerlach, Prog. Inorg. Chem., 26 (1980) 1.
59 P. Pauling, G.B. Robertson and G.A. Rodley, Nature (London), 207 (1960) 73.
60 M. Gerloch, J. Kohl, J. Lewis and W. Urland, J. Chem. Soc. A, (1970) 3283.
61 A. Bencini, C. Benelli, D. Gatteschi and C. Zanchini, Inorg. Chem., 18 (1979) 2526.
62 C.P. Keijzers, G. van Kalkeren, E. de Boer and J.S. Wood, Mol. Phys., 49 (1983) 1187.
63 C. Freibel, J. Pebler, F. Steffens, M. Weber and D. Reinen, J. Solid State Chem., 46 (1983) 253.
64 B.J. Hathaway, P.G. Hodgson and P.C. Power, Inorg. Chem., 13 (1974) 2009.
65 J.H. Ammeter, L. Zoller, J. Bachmann, P. Baltzer, E. Gamp, R. Bucher and E. Deiss, Helv. Chim. Acta, 64 (1981) 1063.
66 B.J. Hathaway, M. Duggan, A. Murphy, J. Mullene, C. Power, A. Walsh and B. Walsh, Coord. Chem. Rev., 36 (1981) 267.
67 D. Reinen and C. Freibel, Struct. Bonding (Berlin), 37 (1979) 1.
68 A. Bencini, C. Benelli and D. Gatteschi, Inorg. Chem., 19 (1980) 1632.
69 D.W. Smith, J. Chem. Soc. A., (1969) 2529.
70 M.A. Hitchman, Inorg. Chem., 11 (1972) 2387.
71 C.J. Ballhausen and E.M. Ancmon, K. Dan. Vidensk. Selsk. Mat.-Fys. Medd., 29 (1954) 4.
72 C. Linares, A. Louat and M. Blanchard, Struct. Bonding (Berlin), 33 (1977) 179.
73 K.D. Warren, Inorg. Chem., 16 (1977) 2008.
74 N. Edelstein, D. Brown and N. Whittaker, Inorg. Chem., 13 (1974) 563.
75 D. Brown, B. Whittaker and N. Edelstein, Inorg. Chem., 13 (1974) 1805.
76 D. Brown, P. Lidster, B. Whittaker and N. Edelstein, Inorg. Chem., 15 (1976) 511.
77 W. Urland, Chem. Phys. Lett., 53 (1978) 296.
78 W. Urland, Chem. Phys. Lett., 77 (1981) 58.

79 W. Urland, Chem. Phys. Lett., 83 (1981) 116.
80 W. Urland, Ber. Bunsenges. Phys. Chem., 85 (1981) 1139.
81 D.A. Cruse and M. Gerloch, J. Chem. Soc., (1976) 1617.
82 B.N. Figgis, M. Gerloch and R. Mason, Acta Crystallogr., 17 (1964) 606.
83 W. DeW. Horrocks and D.A. Burlone, J. Am. Chem. Soc., 98 (1976) 6512.
84 J.A. McGinnety, J. Am. Chem. Soc., 94 (1972) 8406.
85 G.M. Gerloch and M.R. Manning, Inorg. Chem., 20 (1981) 1051.
86 M.R. Manning and P.R. Raithby, in press.
87 J.E. Davies, M. Gerloch and D.J. Phillips, J. Chem. Soc., (1979) 1836.
88 G. Garton, D.E. Henn, H.H. Powell and L.M. Venanzi, J. Chem. Soc., (1963) 3625.
89 A. Bencini, C. Benelli, D. Gatteschi and C. Zanchini, Inorg. Chem., 18 (1979) 2137.
90 J.A. Bertrand and A.R. Klayanaraman, Inorg. Chim. Acta, 5 (1979) 341.
91 M. Gerloch, L.R. Hanton and M.R. Manning, Inorg. Chim. Acta, 48 (1981) 205.
92 P.T. Greem and L. Sacconi, J. Chem. Soc. A, (1970) 866.
93 M. Gerloch and I. Morgenstern-Badarau, J. Chem. Soc. Dalton Trans., (1977) 1619.
94 M.A. Hitchman, J. Chem. Soc. Faraday Trans. 2, (1972) 846.
95 R.P. Van Stapele, H.G. Beljers, P.F. Bongers and H. Zijlstre, J. Chem. Phys., 44 (1966) 3719.
96 B. Morosin and E.C. Lingafelter, Acta Crystallogr., 13 (1960) 807.
97 M. Gerloch and L.R. Hanton, Inorg. Chem., 19 (1980) 1692.
98 A. Bencini and D. Gatteschi, Inorg. Chem., 16 (1977) 2141.
99 A. Bencini, C. Benelli, D. Gatteschi and C. Zanchini, J. Mol. Struct., 60 (1980) 401.
100 W. DeW. Horrocks, D.H. Templeton and A. Zalkin, Inorg. Chem., 7 (1968) 2303.
101 M. Gerloch and L.R. Hanton, Inorg. Chem., 20 (1981) 1046.
102 L.R. Hanton and P.R. Raithby, Acta Crystallogr., Sect. B, 36 (1980) 2417.
103 D.L. Johnson, W.L. Rohrbaugh and W. DeW. Horrocks, Inorg. Chem., 10 (1971) 547.
104 R.J. Butcher and E. Sinn, Inorg. Chem., 16 (1977) 2234.
105 R.P. Taylor, D.H. Templeton, A. Zalkin and W. DeW. Horrocks, Inorg. Chem., 7 (1968) 2624.
106 P. Dapporto and L. Sacconi, J. Chem. Soc. A, (1971) 1914.
107 J.A.J. Jarvis, R.H.B. Mais and P.G. Owsten, J. Chem. Soc. A, (1968) 1473.
108 Van H.L. Schläfer, M. Martin, H.H. Schmidtke, Ber. Bunsenges. Phys. Chem., 75 (1971) 787.
109 J. Glerup, O. Mønsted and C.E. Schäffer, Inorg. Chem., 15 (1976) 1399.
110 T.J. Barton and R.C. Slade, J. Chem. Soc. Dalton Trans., (1975) 650.
111 K. Keeton, B. Fa. Chum Chon and A.B.P. Lever, Can. J. Chem., 49 (1971) 192.
112 A. Bencini, C. Benelli, D. Gatteschi and C. Zanchini, Inorg. Chem., 12 (1983) 2123.
113 D.L. Cullen and E.C. Lingafelter, Inorg. Chem., 9 (1970) 1858.
114 A.B.P. Lever, I.M. Walker and P.J. McCarthy, Inorg. Chim. Acta, 39 (1980) 81.
115 I. Bertini, D. Gatteschi and A. Scozzafava, Inorg. Chem., 14 (1975) 812.
116 M. Di Vaira and P.L. Orioli, Inorg. Chem., 6 (1967) 955.
117 M. Di Vaira and A. Bianchi Orlandini, Inorg. Chem., 12 (1973) 1292.
118 G. Fallani, R. Morassi and F. Zanobini, Inorg. Chim. Acta, 12 (1975) 147.
119 L. Banci, C. Benelli, D. Gatteschi and F. Mani, Inorg. Chem., 21 (1982) 1133.
120 F. Mani and C. Mealli, Inorg. Chim. Acta, 54 (1981) L77.
121 C. Benelli, I. Bertini, M. Di Vaira and F. Mani, Inorg. Chem., in press.
122 R. Dingle and R.A. Palmer, Theor. Chim. Acta, 6 (1965) 249.
123 L.N. Swink and M. Atoji, Acta Crystallogr., 13 (1960) 639.
124 I. Bertini, D. Gatteschi and A. Scozzafava, Inorg. Chem., 15 (1976) 203.

125 B.W. Brown and E.C. Lingafelter, Acta Crystallogr., 16 (1963) 753.
126 L.K. Minacheva, M.A. Porai-Koshits and A.S. Autsyschkina, J. Struct. Chem. (USSR), 10 (1969) 72 (Engl. Transl.).
127 A.F. Schreiner and D.J. Hamm, Inorg. Chem., 12 (1973) 2041.
128 A.B.P. Lever, G. London and P.J. McCarthy, Can. J. Chem., 55 (1977) 3172.
129 D. Gatteschi and A. Scozzafava, Inorg. Chim. Acta, 21 (1977) 223.
130 M.J. Daniello Jr., M.F. Mocella, F. Wagner, K. Barefield and I.C. Paul, J. Am. Chem. Soc., 97 (1975) 192.
131 A.B.P. Lever, I.M. Walker, P.J. McCarthy, K.B. Mertes, A. Jircitano and R. Sheldon, Inorg. Chem., 22 (1983) 2252.
132 I.M. Walker, A.B.P. Lever and P.J. McCarthy, Can. J. Chem., 58 (1980) 823.
133 A.J. Finney, M.A. Hitchman, C.L. Ralston, G.L. Rowbottom and A.H. White, Aust. J. Chem., 34 (1981) 2047.
134 A.B.P. Lever, I.M. Walker and P.J. McCarthy, Inorg. Chim. Acta, 44 (1980) L143.
135 A.B.P. Lever, I.M. Walker and P.J. McCarthy, Can. J. Chem., 60 (1982) 495.
136 M.J. Goldberg and R.E. Marsh, Acta Crystallogr. Sect. B, 35 (1979) 960.
137 D.W. Smith, Inorg. Chem., 17 (1978) 3153.
138 J. Glerup, O. Mønsted and C.E. Schäffer, Inorg. Chem., 19 (1980) 2855.
139 M. Gerloch, R.F. McMeeking and A.M. White, J. Chem. Soc. Dalton Trans., (1975) 2452.
140 I. Søtofte and S.E. Rasmussen, Acta Chem. Scand., 21 (1967) 2028.
141 M. Gerloch and I. Morgenstern-Badarau, Inorg. Chem., 18 (1979) 3225.
142 G.J. Palenik and D.W. Wester, Inorg. Chem., 17 (1978) 864.
143 M. Gerloch, I. Morgenstern-Badarau and J.P. Audiere, Inorg. Chem., 18 (1979) 3220.
144 A. Bencini, C. Benelli, D. Gatteschi and C. Zanchini, Inorg. Chem., 19 (1980) 1301.
145 M.A. Porai-Koshits, Tr. Inst. Kristallogr. Akad. Nauk SSSR, (1955) 19.
146 M. Gerloch, R.F. McMeeking and A.M. White, J. Chem. Soc. Dalton Trans., (1976) 655.
147 R.C. Elder, Inorg. Chem., 7 (1968) 1117.
148 J.T. Haskagen and J.P. Fackler, Jr., J. Am. Chem. Soc., 87 (1965) 2821.
149 C.W. Reimann, A.D. Mighall and F.A. Maner, Acta Crystallogr., 23 (1967) 135.
150 A. Bencini, C. Benelli, D. Gatteschi and C. Zanchini, Inorg. Chem., 22 (1983) 2123.
151 J. Reedijk and P.J. Wan der Put, Int. Conf. Coord. Chem., 16 (1974) 2.27b.
152 A. Santoro, A.D. Mighall, M. Zocchi and C.W. Reimann, Acta Crystallogr., Sect. B, 25 (1969) 842.
153 J. Reedijk and G.C. Verschoor, Acta Crystallogr., Sect. B, 29 (1973) 721.
154 A. Wada, N. Sakahe and J. Tanaka, Acta Crystallogr., Sect. B, 32 (1976) 1121.
155 M. Gerloch and L.R. Hanton, Inorg. Chim. Acta, 49 (1981) 37.
156 M. Gerloch, L.R. Hanton and M.R. Manning, Inorg. Chim. Acta, 48 (1981) 205.
157 W.C. Hamilton, Acta Crystallogr., 15 (1962) 353.
158 A. Bencini, C. Benelli, D. Gatteschi and C. Zanchini, Inorg. Chem., 19 (1980) 3027.
159 B. Morosin, Acta Crystallogr., 22 (1962) 315.
160 H.A. Hitchman, Inorg. Chim. Acta, 26 (1977) 237.
161 M. Calligaris, G. Nardin and L. Randaccio, J. Chem. Soc. Dalton Trans., (1974) 1903.
162 A. Bencini and D. Gatteschi, Inorg. Chem., 16 (1977) 1994.
163 H. Nakai and Y. Deguchi, Bull. Chem. Soc. Jpn., 48 (1976) 2557.
164 H.A. Hitchman and T.D. Waite, Inorg. Chem., 15 (1976) 2150.
165 D.J. Robinson and C.H.L. Kennard, Cryst. Struct. Commun., 1 (1978) 185.
166 A.B.P. Lever, Inorganic Electronic Spectroscopy, Elsevier, Amsterdam, 2nd edn., 1968.
167 D.J. Mackey, S.V. Evans and R.F. McMeeking, J. Chem. Soc. Dalton Trans., (1978) 160.

168 T.J. Bergendhal and J.S. Wood, Inorg. Chem., 14 (1974) 338.
169 M. Vijayan and M.A. Vismamitra, Acta Crystallogr., 21 (1964) 522.
170 A. Bencini, C. Benelli, D. Gatteschi and C. Zanchini, Inorg. Chem., 19 (1980) 3829.
171 I. Bertini, P. Dapporto, D. Gatteschi and A. Scozzafava, Inorg. Chem., 14 (1975) 1639.
172 D.J. MacKey and R.F. McMeeking, J. Chem. Soc. Dalton Trans., (1977) 2168.
173 W. DeW. Horrocks and D.A. Burlone, Inorg. Chim. Acta, 35 (1979) 165.
174 M.R. Fox, P.L. Orioli, P. Paoletti and M. Ciampolini, Acta Crystallogr., 17 (1964) 1159.
175 C. Benelli, D. Gatteschi and G.P. Speroni, Inorg. Chim. Acta, in press.
176 P.L. Orioli, L. Sacconi and M. Di Vaira, Chem. Commun., 1 (1965) 103.
177 M.A. Hitchman, Inorg. Chem., 16 (1977) 1985.
178 W.P. Schaeffer and R.E. Marsh, Acta Crystallogr., Sect. B, 25 (1969) 1675.
179 R. De Iasi, S.L. Holt and B. Port, Inorg. Chem., 10 (1971) 1498.
180 M. Calligaris, D. Minichelli, G. Nardin and L. Randaccio, J. Am. Chem. Soc. A, (1970) 2411.
181 G.R. Clark, D. Hall and T.N. Waters, J. Chem. Soc. A, (1969) 823.
182 D.A. Cruse and M. Gerloch, J. Chem. Soc., (1977) 1613.
183 P.L. Orioli, M. Di Vaira and L. Sacconi, J. Am. Chem. Soc., 88 (1966) 4383.
184 D.A. Cruse and M. Gerloch, J. Chem. Soc., (1977) 152.
185 M.B. Hursthause, K.M.A. Malik, J.E. Davies and J.H. Harding, Acta Crystallogr., Sect. B, 34 (1978) 1355.
186 M.A. Hitchman, Inorg. Chem., 13 (1974) 2218.
187 L. Falvello and M. Gerloch, Inorg. Chem., 19 (1980) 472.
188 L. Falvello and M. Gerloch, Acta Crystallogr., Sect. B, 35 (1979) 2547.
189 A. Bencini, C. Benelli, D. Gatteschi and L. Sacconi, Inorg. Chim. Acta, 37 (1979) 195.
190 P. Dapporto, G. Fallani and L. Sacconi, Inorg. Chem., 13 (1974) 2847.
191 K.W. Penfield, R.R. Gay, R.S. Himmelwright, N.C. Eickman, V.A. Norris, H.C. Freeman and E.I. Solomon, J. Am. Chem. Soc., 103 (1981) 4382.
192 P.J. Colman, H.C. Freeman, J.M. Guss, M. Murata, C.A. Norris, J.A.M. Ramshaw and M.P. Venkatappa, Nature (London), 272 (1978) 319.
193 D.W. Smith, Struct. Bonding (Berlin), 12 (1972) 49.
194 W.E. Hatfield and T.S. Piper, Inorg. Chem., 3 (1964) 841.
195 D.W. Smith, J. Chem. Soc. A, (1969) 1978.
196 D.L. McFadden, A.J. McPhail, C.D. Garner and F.E. Mabbs, J. Chem. Soc. Dalton Trans., (1976) 47.
197 D.L. McFadden, A.J. McPhail, C.D. Garner and F.E. Mabbs, J. Chem. Soc. Dalton Trans., (1975) 263.
198 M.P. Byrn, B.A. Katz, N.L. Nader, K.R. Lavan, C.J. Maguarney, K.N. Miller, J.W. Pritt and C.E. Strouse, J. Am. Chem. Soc., 105 (1983) 4916.
199 W.T. Oosterhuis and G. Lang, Phys. Rev., 178 (1969) 439.
200 C. Creutz and H. Taube, J. Am. Chem. Soc., 91 (1969) 3988.
201 M. Robin and P. Day, Adv. Inorg. Chem. Radiochem., 10 (1967) 248.
202 B.C. Burker, R.S. Drago, D.N. Hendrickson, R.M. Richman and S.L. Kessel, J. Am. Chem. Soc., 100 (1978) 3805.
203 N.S. Hush, A. Edgar and J.K. Beattie, Chem. Phys. Lett., 69 (1980) 128.
204 U. Fürholz, H.B. Bürgi, F.E. Wagner, A. Stebler, J.H. Ammeter, E. Kransz, R.J. Clark, M.J. Stead and A. Ludi, J. Am. Chem. Soc., 106 (1984) 121.